NASA TM - 80163

NASA Technical Memorandum 80163

NASA-TM-80163 19800001985

COMPARISON OF STABILITY AND CONTROL PARAMETERS FOR A LIGHT, SINGLE-ENGINE, HIGH-WINGED AIRCRAFT USING DIFFERENT FLIGHT TEST AND PARAMETER ESTIMATION TECHNIQUES

William T. Suit and Robert L. Cannaday

September 1979

NASA
National Aeronautics and
Space Administration

Langley Research Center
Hampton, Virginia 23665

COMPARISON OF STABILITY AND CONTROL PARAMETERS FOR A LIGHT, SINGLE-ENGINE, HIGH-WINGED AIRCRAFT USING DIFFERENT FLIGHT TEST AND PARAMETER ESTIMATION TECHNIQUES

William T. Suit and Robert L. Cannaday

SUMMARY

Longitudinal and lateral stability and control parameters were estimated from flight data for a high-wing, general aviation, airplane using flight data obtained at various flight conditions within the normal range of the aircraft. These parameters were estimated using an output error technique (maximum likelihood) and an equation error technique (linear regression). Longitudinal static parameters were also estimated from climbing, descending, and quasi-steady-state flight data. For the lateral excitations, four input forms were used involving some combination of rudder and ailerons. The resulting longitudinal and lateral parameter estimates were used to compute the periods and time-to-damp to one-half amplitude of the various aircraft modes of motion to determine the sensitivity of these motions to variations in the parameter estimates.

INTRODUCTION

The use of simulators for research investigations into aircraft dynamics is becoming an increasingly important tool of the research engineer. With this increased use of simulations comes the demand for greater simulator fidelity, which requires improved mathematical models. The aerodynamics of an aircraft can be described mathematically using its stability and control parameters in a set of equations of motion.

Several techniques have been used in the past to estimate stability and control parameters from flight data including analog matching (refs. 1 and 2), the time vector method (ref. 1), and regression analysis (refs. 3 and 4). In recent years the estimation of parameters from flight data by use of a maximum-likelihood algorithm (ref. 5) has become fairly routine where adequate computer facilities are available. In general, the analyses reported in these references were based on the small perturbation equations of motion.

To date, stability and control parameters for several low-winged light airplanes have been determined from both flight test data and wind-tunnel tests (refs. 6, 7, 8, and 9). For high-winged configurations wind tunnel test data are available (ref. 10) but little has been published on the estimated values of stability and control parameters determined from flight data. Wind tunnel tests usually do not include estimated values for rotary derivatives, which can be estimated from flight test data using current estimation techniques.

The present paper is similar in some respects to the work that was done for the low-winged, general aviation aircraft as reported in references 7 and 8. However, in the present study, flight test data were obtained at three different airspeeds corresponding approximately to landing, approach, and cruise conditions. During the flight test, the aircraft was perturbed from trim conditions using either elevator or rudder and ailerons, and the stability and control parameters were estimated from the resulting data using both an output error method (maximum likelihood of ref. 5), and an equation error method (linear regression of refs. 3 and 11). Static longitudinal aerodynamic parameters were also calculated from steady climb, descent, and quasi-steady flight data for comparison with those obtained from perturbation flight data.

This report describes the flight test procedure, presents the results obtained from the perturbation flight tests using the two estimation procedures, and compares values for the longitudinal static parameters with values calculated from independent flight tests at two different center-of-gravity locations.

SYMBOLS

The aerodynamic parameters are referenced to a system of body axes with the origin at the airplane center of gravity, which is located at 28.8 percent $\bar{c}$, and with orientation of body axes as shown in figure 1, which also shows the direction of positive forces, moments, displacements, angles, and linear and angular velocities.

a_X, a_Y, a_Z	acceleration measured along X, Y, and Z body axes, respectively, g units
b	wing span, m
$\bar{c}$	wing mean geometric chord, m
F_X, F_Y, F_Z	force along X, Y, and Z body axes, respectively, N
g	acceleration due to gravity, m/sec^2
I_X, I_Y, I_Z	moment of inertia about X, Y, and Z body axes, respectively, kg-m^2
I_{XZ}	product of inertia, kg-m^2
l_t	distance from airplane center of gravity to center of pressure of horizontal tail, m
M_X, M_Y, M_Z	rolling, pitching, and yawing moments, respectively, N-m
m	mass, kg

p	roll rate, rad/sec
q	pitch rate, rad/sec
$\bar{q}$	dynamic pressure, N/m^2
r	yaw rate, rad/sec
R	estimate of error covariance matrix
S	wing area, m^2
T	thrust, N
u, v, w	velocity along X, Y, and Z body axes, respectively, m/sec
u', v', w'	velocity component along X, Y, and Z body axes, respectively, at angle-of-attack sensor on wing-tip boom, m/sec
U	control vector
V	airplane total velocity, m/sec
X_i	matrix of measured states and input variables
X, Y, Z	body coordinate axes through airplane center of gravity
$x(i)$	state vector
$y(i)$	output vector
$\bar{x}$, $\bar{y}$, $\bar{z}$	x-, y-, and z-coordinates, respectively, of the sensors on wing-tip boom relative to airplane center of gravity, m
z_i	measurement vector
α	angle of attack, rad
β	angle of sideslip, rad
δ_a	left aileron deflection minus right aileron deflection, rad
δ_e	stabilator deflection, positive trailing edge down, rad
δ_r	rudder deflection, positive trailing edge left, rad
ϵ	angle between thrust axis and airplane X body axis, positive for thrust up, rad
θ	pitch angle, rad

θ	parameter vector
ρ	air density, kg/m^3
η	measurement noise vector
φ	roll angle, rad
Δ	perturbation in parameter vector
C_L	lift coefficient, $gm/\bar{q}S$
C_{ℓ}	rolling-moment coefficient, $M_X/\bar{q}Sb$
C_m	pitching-moment coefficient, $M_Y/\bar{q}S\bar{c}$
C_n	yawing-moment coefficient, $M_Y/\bar{q}S\bar{c}$
C_T	thrust coefficient, $T/\bar{q}S$ (used in some publications as T'_c)
C_X	axial-force coefficient, $F_X/\bar{q}S$
C_Y	side-force coefficient, $F_Y/\bar{q}S$
C_Z	normal-force coefficient, $F_Z/\bar{q}S$

$$C_{\ell_p} = \frac{\partial C_\ell}{\partial \frac{pb}{2V}} \qquad C_{\ell_r} = \frac{\partial C_\ell}{\partial \frac{rb}{2V}} \qquad C_{\ell_\beta} = \frac{C_L}{\beta} \qquad C_{L_\alpha} = \frac{\partial C_L}{\partial \alpha}$$

$$C_{\ell_{\delta a}} = \frac{\partial C_\ell}{\partial \delta_a} \qquad C_{\ell_{\delta r}} = \frac{\partial C_\ell}{\partial \delta_r} \qquad C_{m_q} = \frac{\partial C_m}{\partial \frac{q\bar{c}}{2V}} \qquad C_{m_\alpha} = \frac{\partial C_m}{\partial \alpha}$$

$$C_{m_{\dot{\alpha}}} = \frac{\partial C_m}{\partial \frac{\dot{\alpha}\bar{c}}{2V}} \qquad C_{m_{\delta e}} = \frac{\partial C_m}{\partial \delta_e} \qquad C_{n_p} = \frac{\partial C_n}{\partial \frac{pb}{2V}} \qquad C_{n_r} = \frac{\partial C_n}{\partial \frac{pb}{2V}}$$

$$C_{n_\beta} = \frac{\partial C_n}{\partial \beta} \qquad C_{n_{\delta a}} = \frac{\partial C_n}{\partial \delta_a} \qquad C_{n_{\delta r}} = \frac{\partial C_n}{\partial \delta_r} \qquad C_{T_\alpha} = \frac{\partial C_T}{\partial \alpha}$$

$$C_{X_\alpha} = \frac{\partial C_X}{\partial \alpha} \qquad C'_{X_\alpha} = C_{X_\alpha} + C_{T_\alpha} \cos \epsilon \qquad C_{Y_p} = \frac{\partial C_Y}{\partial \frac{pb}{2V}} \qquad C_{Y_r} = \frac{\partial C_Y}{\partial \frac{rb}{2V}}$$

$$C_{Y_\beta} = \frac{\partial C_Y}{\partial \beta} \qquad C_{Y_{\delta r}} = \frac{\partial C_Y}{\partial \delta_r} \qquad C_{Z_q} = \frac{\partial C_Z}{\partial \frac{q\bar{c}}{2V}} \qquad C_{Z_\alpha} = \frac{\partial C_Z}{\partial \alpha}$$

$$C'_{Z_\alpha} = C_{Z_\alpha} + C_{T_\alpha} \sin \epsilon \qquad C_{z_{\delta e}} = \frac{\partial C_Z}{\partial \delta_e} \qquad C_{T_\alpha} = \frac{\partial C_T}{\partial \alpha}$$

Subscripts:

c	computed
k	index
m	measured
o	coefficient at trimmed conditions
t	trimmed conditions

Superscripts:

-1	inverse matrix
T	transpose matrix
M	measured quantity
o	nominal evaluation
^	estimated value

A dot over a symbol signifies a derivative with respect to time.

DESCRIPTION OF AIRPLANE AND DATA SYSTEM

The subject airplane was a four-place, externally braced high-wing, fixed tricycle landing gear, single-engine airplane, as shown in figure 2. Its pertinent geometric details and mass characteristics are given in table I. The mass characteristics shown were obtained from manufacturer's data on the subject aircraft. The airplane instrumentation used to record control-surface movements and airplane responses to these movements was basically like that of the subject aircraft of reference 7.

The instrumentation system measured and recorded on tape the data used in this study. The variables recorded and the range of each sensing instrument is given in table II. The accuracy of these measurements is considered to be 2 or 3 percent of full scale on each instrument. Unlike the data recorded in reference 7 in which FM and PAM were merged, all the data were recorded on FM (continuous) channels. The advantage of this was that all data channels could be filtered using an analog filter without introducing time delays in some channels relative to others. These data were digitized, then sampled at 20 points per second and converted to engineering units to obtain the data used in this study. The pitot-static head for measuring velocity (dynamic pressure), and the angle-of-attack and angle-of-sideslip vanes were mounted on a boom located near the left wing tip. The boom extended 3/4 chord ahead of the wing leading edge.

FLIGHT TESTS

Three types of flight tests were flown to obtain the data used in this report.

(1) Perturbation tests.- These tests consisted of trimming the airplane with power for level flight, idle, or full power and perturbing the trimmed condition with either elevator or rudder and aileron doublets. A typical time history of the input forms used to excite the longitudinal motions is presented in figure 3. The aircraft was trimmed at three indicated airspeeds; 31.6 m/sec (61 knots), 40.7 m/sec (78 knots), and 54.2 m/sec (104 knots), which correspond roughly to landing, approach, and cruise, although no flaps were used in these tests.

The lateral perturbation tests consisted of trimming the aircraft at the same three airspeeds as for the longitudinal data, but only trim power for level flight was used. Four different input forms designated A, B, C, and D, were used to excite the lateral motions, and typical time histories of the inputs are illustrated in figure 3. All perturbation data were obtained for one center-of-gravity (c.g.) location, 28.8 percent MAC, and test altitudes ranged from about 600 m to 1500 m in relatively smooth air.

The number of test runs made at each condition longitudinally and laterally and for each input is presented in table III.

(2) Steady tests.- These tests consisted of trimming the airplane for a steady full power climb for a particular airspeed followed by setting the power to idle and trimming for an idle power steady descent at the same airspeed and altitude range as the climb. This test was done for the same three airspeeds as above, with no flap deflection, and two c.g. locations 28.8 percent MAC, and 36.5 percent MAC. No analysis for lateral characteristics was performed on these data.

(3) Quasi-steady tests.- These tests consisted of performing slow acceleration-deceleration flight test maneuver (ref. 12), starting from trimmed level flight. Power for these tests was left at the trim setting. The initial trimmed indicated airspeeds were again 31.6 m/sec (61 knots), 40.7 m/sec (78 knots), and 54.2 m/sec (104 knots). These tests were performed at the same c.g. locations as the steady tests. No flaps were used nor was an analysis of lateral characteristics made for these data.

DATA REDUCTION AND ESTIMATION METHODS

The measured flight data included dynamic pressures, angles of attack and sideslip, linear accelerations, rotational rates, and control surface movements. It was necessary to apply corrections to the measured flight data before it could be used for estimating stability and control parameters. Since the angle of attack and sideslip vanes were mounted on a boom located near the left wing tip and extended about 3/4 chord ahead of the wing leading edge, corrections for upwash and angular rates were applied to the measured angle-of-attack. Angle-of-sideslip was corrected for angular rates. Details of the angle-of-attack and sideslip corrections are given in reference 7. Airspeed was corrected for position error by applying a correction to the static pressure determined from an airspeed calibration test. The airspeed was also corrected for altitude to obtain true airspeed, and since the pitot head was located on the boom, angular rates were taken into account to convert airspeed to the aircraft c.g. (ref. 7). The accelerometer readings were also corrected to the c.g. of the airplane.

Three methods were used to estimate stability and control parameters using the corrected flight test data. These were the maximum likelihood technique described in reference 5, a regression parameter estimation technique described in references 3 and 11, and an analytical technique described in reference 13.

The maximum likelihood technique utilizes the log-likelihood function

$$J(\Theta) = -1/2 \sum \eta_i^T R^{-1} \eta_i - \frac{N}{2} \log|R|$$

where

$$\eta_i = z_i - \hat{y}_i = y_i - y_i(\Theta_o) - \left.\frac{\partial y_i}{\partial \Theta}\right|_{\Theta = \Theta_o} \Delta\Theta$$

with z_i the measurement vector and y_i the output vector which comes from $\dot{x} = f(x, U, \Theta, t)$ and $y = g(x, U, \Theta, t)$. In the above equation η_i is assumed to have a Guassian distribution and the representation $\dot{x} = f(x, U, \Theta, t)$ is assumed to accurately represent the physical system. The unknowns to be estimated are the elements of Θ and R. Minimizing J with respect to R, $\hat{R} = \text{diag}\ \frac{1}{N} \sum_i \eta_i\ \eta_i^T$ is obtained. The estimates for the parameters are obtained from the equation

$$\left.\frac{\partial J}{\partial \Theta}\right|_{\Theta=\hat{\Theta}} = 0$$

which results in

$$\Delta\hat{\theta} = \left[\sum_i \left(\frac{\partial y_i}{\partial \theta}\right)^T \hat{R}^{-1} \frac{\partial y_i}{\partial \theta}\right]^{-1} \left[\sum_i \frac{\partial y_i}{\partial \theta} \hat{R}^{-1} \eta_i\right]$$

yielding the parameter estimates

$$\hat{\theta} = \theta_o + \Delta\theta$$

The regression technique utilizes the cost function

$$J_r(\theta) = \sum_{i=1}^{N} \left[\dot{x}_{ri} - f_{ri}(x, U, \theta_r)\right]^2$$

where r indicates the rth state equation.

The estimates of the unknown parameters are obtained from the equation

$$\frac{\partial J}{\partial \theta} = 0$$

which results in

$$\hat{\theta} = \left[\sum_i X_i^T X_i\right]^{-1} \left[\sum_i X_i^T \dot{x}_{ri}\right]$$

where the matrix X_i includes measured states and output variables (assumed noise free).

The analytical technique was used to determine the longitudinal static and control parameters. These were estimated using the measured stick-fixed trim curves at two c.g. positions and the measured C_L as a function of angle-of-attack curve. C_{L_α} was determined using the slope of the C_L versus α curve. C_{m_α} was determined from the slopes of the stick-fixed trim curves. $C_{m_{\delta e}}$ was determined using the difference between the stick-fixed trim curves for various C_L's. $C_{Z_{\delta e}}$ was then calculated from $C_{m_{\delta e}}$ (see relation in appendix).

The application of these techniques is outlined in figure 4. The maximum likelihood and regression techniques were applied to the perturbation data, and the analytical technique of reference 13 was applied to the steady and quasi-steady data.

One criterion used to evaluate the uncertainty of the parameter estimates obtained using the maximum-likelihood technique is the Cramer-Rao bound discussed in reference 14. The Cramer-Rao bounds are an estimate of the standard deviations of the parameter estimates but they are too small except for the ideal case of a perfect mathematical model, infinite data points, and unbiased random noise in the data. Since this is not the case in a practical situation, the Cramer-Rao bounds can be used in a relative sense to determine the estimation accuracy.

The effects of power settings on the estimated parameters were determined by comparing the values of the estimated parameters determined using full power data with those determined using idle power data.

RESULTS AND DISCUSSION

Longitudinal

The results of applying the various estimation techniques to the longitudinal flight data are shown in figure 5. The longitudinal parameters estimated for each longitudinal run are also given in table IV. All of the parameters except C_{z_q} and $C_{z_{\delta e}}$ had Cramer-Rao bounds less than 2 percent of the estimated value (table V). These results indicate that the uncertainty in the estimated values was small. Where repeat runs were available, the longitudinal parameter values estimated by both methods agreed to within 10 percent of each other in the majority of the cases. Also, the fit to the flight data using the maximum likelihood method was considered good since the mean-squared-fit error (area between measured and computed time histories) for each of the states was less than 1 percent of the full-scale range of the instrument used to measure that state. A typical comparison of measured and predicted flight data time histories is shown in figure 6.

The trends of the estimated parameters with C_L were consistent with those approximated from reference 10 where comparisons could be made. The values determined by both the maximum likelihood and the linear-regression methods generally showed similar trends. The left half of figure 5 shows the parameters estimated from data which were obtained by perturbing the aircraft from trim powered level flight while the right half shows parameters estimated from data taken when the aircraft was perturbed from idle or full powered flight. The curves fared through the points determined using the maximum likelihood estimation method represent the estimates of the derivatives over the C_L range for which flight data were available. Derivatives determined by other methods were shown for comparison, but the values determined using maximum likelihood were considered the most reliable.

C_{x_α}

C_{x_α} was positive and increased linearly with C_L. This trend seems reasonable since C_{x_α} was approximately proportional to C_L (ref. 15). There was a small power effect at the smallest and middle C_L values tested.

C_{z_α}

C_{z_α} was approximately constant with C_L, as was expected, since C_L varies linearly with α in the α range covered by the flight tests (fig. 5). The power effect observed, idle power giving the least negative value, was greatest at the largest C_L values. The same trends can be seen in the results for both the maximum likelihood and the regression extracted methods.

Values of C_{z_α} for full power, trim power for level flight, and idle power were calculated by the techniques of reference 13 using the quasi-steady and steady measurements and the values of C_{z_α} are shown on figure 5. The values of C_{z_α} determined from the steady measurements taken at full power and trim power were about the same, and these values of C_{z_α} were more negative than those extracted from the perturbation tests. The C_{z_α} values calculated by the methods of reference 13 from the steady measurements taken at idle power, were approximately the same as the values estimated from the perturbation test data taken at idle power.

The power effect on the estimated values of C_{z_α} from steady measurements was about 20 percent for this parameter. The power effect on the values estimated using maximum likelihood was about 12 percent. As C_L was decreased, the difference in the estimated values at C_{z_α} for full and idle power decreased for both the perturbation and steady measurements. However, the values of C_{z_α} determined from the steady measurements indicated a larger power effect for all C_L values tested.

Reference 10 describes wind tunnel tests on a high-winged, single-engine airplane. Although the configuration tested in the wind tunnel was not exactly the same as the configuration of the airplane discussed in this report, the two aircraft are somewhat similar. The data in reference 10 indicates that $-C_{z_\alpha}$ ($C_{L_\alpha} \approx -C_{z_\alpha}$) becomes greater as power increases. With the throttle in the idle position in flight, thrust was approximately zero, so this case was considered to be comparable with the $T_c' = 0$ case of reference 10. The thrust coefficient for the full power flight condition was approximately the same as the $T_c' = 0.26$ case of reference 10. The $-C_{z_\alpha}$ of reference 10 for a $T_c' = 0.26$ is about 14 percent greater than the $-C_{z_\alpha}$ value for $T_c' = 0$.

A similar change was noted for the $-C_{z_\alpha}$ estimated from flight data using the maximum likelihood technique. No reqson has been found for the differences in power effects for the values of C_{z_α} determined from the perturbation and steady measurements. However, the power effects seen in the results from the perturbation tests are of the same magnitude as those seen in the wind tunnel test results, so the effect of power on C_{z_α} for the maximum likelihood estimated results were considered reasonable.

C_{z_q}

The magnitudes estimated for C_{z_q} and its trend with C_L differed greatly for the maximum likelihood and the regression estimation methods. Since the parameter had a Cramer-Rao bound at least three times greater than the bound for any of the other estimated parameters C_{z_q} was not considered well determined. Therefore, the estimated value, regardless of its magnitude, did not significantly affect the calculated motions of the aircraft. This can be seen by examining the period and time to damp to half amplitude of the short period mode (table VI).

While the actual values of all the longitudinal parameters estimated by the maximum likelihood and linear regression methods are different, both sets give reasonable fits to the flight data. For representative sets of flight data the periods and times to damp to half amplitude for the short period mode are shown as table VI. The quantities in the table were calculated using the sets of parameters determined by examining a particular set of data with both the maximum likelihood and regression methods. The difference between the periods and times to half were around 10 percent in most cases so that even though the individual derivatives in the mathematical model describing the aircraft were different the resulting motions were similar.

$C_{z_{\delta e}}$

The values estimated for $C_{z_{\delta e}}$ using both the maximum likelihood and the regression techniques were similar even though different mathematical models were used during the estimation procedure. The maximum likelihood mathematical model used a constraint equation which calculated values of $C_{z_{\delta e}}$ from the estimated value of $C_{m_{\delta e}}$ (see refs. 6 and 7). There were no constraints in the regression mathematical model. For the full and idle power cases the magnitudes of the estimated parameters were about the same and there were no obvious differences in the trends with C_L between the two estimation methods. The trend with C_L seemed somewhat different for the two estimation methods when the trim power case was examined, but the magnitudes of the parameters were similar (see fig. 5).

C_{m_α}

The estimated values of C_{m_α} became more negative with increasing C_L (fig. 5). The trends for C_{m_α} were the same for both extraction methods, but the values determined by the maximum likelihood method were more negative. The results showed a definite power effect on C_{m_α} for the higher C_L values, increasing the power tended to make the values of C_{m_α} less negative.

The estimated values were compared with values calculated from the steady and quasi-steady measurements using the methods of reference 13. As can be seen from figure 5, the values of C_{m_α} calculated from quasi-steady measurements showed similar trends and magnitudes as the results of the maximum likelihood estimation.

$C_{m_q} + C_{m_{\dot\alpha}}$

The values of $C_{m_q} + C_{m_{\dot\alpha}}$ for the full power case tended to be more negative as C_L increased (fig. 5). Otherwise there was very little variation with C_L. Both parameter estimation methods showed the similar trends and magnitudes. The values obtained using the regression method tended to be more negative.

A definite power effect was observed, especially at the largest C_L. This was expected since the dynamic pressure ratio at the tail was greater at full power for the largest C_L than at full power for the lower C_L's.

$C_{m_{\delta e}}$

The values of $C_{m_{\delta e}}$ determined from perturbation data became more negative as C_L increased for both the trim and full power cases and for both extraction methods (fig. 5). This increased elevator effectiveness at higher C_L values is due to a higher dynamic pressure ratio at the tail for trimmed and full power than for the lower C_L values. The results from the idle power tests showed that $C_{m_{\delta e}}$ remained approximately constant with increasing C_L (fig. 5), which would be expected since the propeller slipstream is minimal at idle power. The effect of power is similar to that noted for $C_{m_q} + C_{m_{\dot\alpha}}$, the effect of power being greater at the larger C_L.

The values determined using the quasi-steady measurements and maximum likelihood estimation showed similar trends with C_L. For the trim power case the $C_{m_{\delta e}}$ determined from the quasi-steady measurements showed a much larger variation with increasing C_L than the $C_{m_{\delta e}}$ determined from the maximum likelihood estimates.

Lateral

The lateral derivatives estimated by the maximum likelihood method are shown on figure 7. A linear fit to each set of these derivatives is also shown on figure 7. Values from this linear fit to the derivatives determined by maximum likelihood are the preferred values to be used to mathematically represent the subject aircraft within the flight regimes covered by the tests. Other values are presented for comparison with the values determined using maximum likelihood. The lateral derivatives estimated by the linear regression method are shown on figure 8. The individual parameters for each run as estimated by each method are given as tables VII and VIII. The run numbers are shown on the tables to enable the reader to compare the results of applying each method to the same data. For comparison the linear fit to each of the maximum likelihood derivatives was also shown on the plot of the corresponding derivatives as determined using the linear regression method (see fig. 8). The derivative values determined by both methods in general showed similar trends and in most cases had similar magnitudes. As another comparison of the maximum likelihood and equation error parameter estimates, the characteristics of the dutch roll, roll, and spiral modes were computed based on the two sets of estimates. These computed characteristics are shown in table IX. The characteristics estimated are similar for parameters obtained from both techniques. The most obvious discrepancy is in the description of the spiral mode, but these differences are not considered important since the data runs were not long enough to accurately describe the spiral mode.

Where possible the trends of the parameter values determined using maximum likelihood were also compared with trends obtained from references 10 and 16. Also, the estimated parameter values will be compared with values taken from reference 17. These are given in table X. The derivative values shown are for a high-winged, single-engine, general aviation aircraft, but only the values from reference 17 are for the specific configuration of this report.

The Cramer-Rao bounds of the lateral derivatives estimated were examined and C_{y_β}, C_{ℓ_β}, C_{ℓ_p}, $C_{\ell_{\delta a}}$, C_{n_β}, C_{n_r}, and $C_{n_{\delta r}}$ were found to have bounds that were less than 2 percent of the extracted values (table XI). An examination of figures 7 and 8 reveals that the derivatives listed above had the least scatter, as would be expected since the Cramer-Rao bounds were small. In most cases, the derivatives C_{y_r}, $C_{y_{\delta r}}$, C_{ℓ_r}, and C_{n_p} had Cramer-Rao bounds of less than 5 percent of the estimated values, the derivatives $C_{\ell_{\delta r}}$, and $C_{n_{\delta a}}$ had a Cramer-Rao bounds of less than 10 percent of the estimated values, and C_{y_p} had a Cramer-Rao bound which varied considerably from run to run. The derivatives with Cramer-Rao bounds of 5 percent or less of the estimated value were considered well determined. Also, the fit to the flight data was considered good since the mean squared fit error for each state was less than 1 percent of the full scale range of the instrument used to measure that state. A typical fit to the lateral motions is shown in figure 9.

No apparent effect of control input was seen in the values obtained using the maximum likelihood estimation method. However, when the linear regression estimation method was used, several of the parameters showed some effect of input form (see fig. 10). With the exception of C_{y_β} and C_{ℓ_r} none of the parameters that were considered well determined showed an effect of input. The values estimated for C_{y_β} from the data generated when input B was used to perturb the aircraft were consistently less negative than when the data generated by the other inputs were used. Some of the parameters that were not as well determined also had apparent input effects for some C_L's, but the scatter in the values estimated by the linear regression method made a definite conclusion difficult.

The reasons for input effects occurring when the linear regression method was used and for their absence when using the maximum likelihood method was used is unclear. One clue may be in the fact that the cost functions are defined differently for the two methods. In the linear regression method, the unknown parameters are estimated for each state equation independently of the other state equations. So, when using linear regression, since the individual inputs excite each of the states in a different manner, several parameter values could be estimated to describe the same state. For the maximum likelihood method all the states to be fitted are estimates simultaneously and the unknown parameter values are determined to give a best overall fit to all the states simultaneously.

The parameters $C_{y_{\delta r}}$, C_{ℓ_β}, C_{ℓ_p}, $C_{\ell_{\delta a}}$, C_{n_β}, and C_{n_p} showed good agreement between the estimation methods (figs. 7 and 8). These parameters had trends with C_L similar to those seen in references 16 and 17 where comparisons could be made. With the exception of C_{ℓ_β} and C_{n_β}, the estimated values agreed with the values shown in table XI from other references. The lateral parameters which had differences between the values determined by maximum likelihood and the values determined by the other methods will now be discussed individually.

C_{y_β}

C_{y_β} was negative and became less negative as C_L increased. The maximum likelihood results showed no effect of control input and the scatter was small. The results using linear regression were less negative than the maximum likelihood results and the scatter was greater. The general trend for the C_{y_β} values extracted by the linear regression method was the same as for the maximum likelihood method, but the linear regression showed some effect of input for input B.

C_{y_p}

C_{y_p} was not determined well by either estimation method as was indicated by the scatter of the estimated values. When using the linear regression program, particularly large run to run variations were noted for the runs with input B.

C_{ℓ_r}

The values estimated for C_{ℓ_r} were positive and increased with increasing C_L. This trend was similar to the trends shown in reference 17, but the magnitudes were lower than expected. The values determined by the linear regression showed the same trend as the maximum likelihood but the values estimated for the parameters were larger. For both estimation methods the values determined using the data for input A were generally lower at the larger C_L's than those determined using the data from the other inputs.

$C_{\ell_{\delta r}}$

The values estimated for $C_{\ell_{\delta r}}$ were positive and increased with increasing C_L. Both the maximum likelihood and linear regression estimation methods generally resulted in similar trends and magnitudes for the estimated parameter. The exception was the values estimated from the data obtained from input A using the regression method. These values tended to show a decrease in $C_{\ell_{\delta r}}$ with increasing C_L.

The general trends seen in the estimated values of $C_{\ell_{\delta r}}$ are opposite those indicated in reference 16 for a straight-winged aircraft. Also, the values estimated were smaller than the value determined from reference 17 and shown in table X. However, since $C_{\ell_{\delta r}}$ is not a strong parameter and is not well determined, the apparent discrepancy did not significantly affect the fit to the data or the other parameter values estimated.

C_{n_r}

The C_{n_r} values which were estimated by both methods were negative and in general the trend of the derivative values was more negative as C_L increased. While both extraction methods gave similar overall trends and scatter for the estimated derivatives some effect of input was seen in the regression results for input D which showed a reverse trend with C_L and for input A which tended to have values less negative than for the other inputs. The scatter in the data hid any possible input effect in the maximum likelihood results. When compared to the values given in table X, the magnitudes of C_{n_r} estimated seemed reasonable and reference 16 implies that the trend with C_L is reasonable.

$C_{n_{\delta a}}$

The values determined for $C_{n_{\delta a}}$ were generally negative, indicating an apparent proverse yaw with aileron deflection for the sign convention used in this report. Experience with the subject aircraft has demonstrated that this aircraft actually has adverse yaw with ailerons. This apparent contradiction can be explained in part when it is realized that the inputs required to determine $C_{n_{\delta a}}$ also produce considerable rolling motion. This rolling motion induces a yawing moment described by the parameter C_{n_p}. Thus, the same aileron inputs which cause a yawing moment through $C_{n_{\delta a}}$, also produce a rolling motion which causes a yawing moment through C_{n_p}. Therefore, the effects described by these two parameters is difficult to separate, as is indicated by the high correlation (.95) between this pair of parameters. This implies that both parameters are required to properly describe the adverse yawing motion observed for the subject aircraft, and not $C_{n_{\delta a}}$ or C_{n_p} alone.

CONCLUDING REMARKS

The maximum likelihood and a linear regression parameter extraction program were used to determine the longitudinal stability and control parameters from data taken using a high-winged, general aviation aircraft. The parameter values obtained using the maximum likelihood method were considered the most reliable representation of the subject aircraft, while the values determined by other methods are presented for comparison.

The longitudinal parameters estimated using maximum likelihood showed the trends expected with variations of power and C_L and were considered to give a reasonable mathematical representation of the aircraft. For a majority of the parameters the same trends were apparent using the linear regression method. A definite effect of power setting was observed in the derivatives $C_{z_{\delta e}}$, C_{m_α}, $C_{m_q} + C_{m_{\dot\alpha}}$, and $C_{m_{\delta e}}$; with some power effects observed in C_{z_α} at the largest C_L. The values estimated for C_{z_α}, C_{z_q}, $C_{z_{\delta e}}$, C_{m_α}, and $C_{m_q} + C_{m_{\dot\alpha}}$ were noticeably different when different parameter estimation methods were used. The parameter $C_{m_{\delta e}}$ showed a lesser variation with estimation method. Also, the derivatives C_{x_α}, $C_{z_{\delta e}}$, C_{m_α}, $C_{m_q} + C_{m_{\dot\alpha}}$, and $C_{m_{\delta e}}$ varied with C_L.

The parameters C_{z_α}, C_{m_α}, and $C_{m_{\delta e}}$ were compared with values determined using steady and quasi-steady test data. The trends with C_L were the same for these derivatives regardless of the method of determination, but the magnitudes were different. The greatest differences were observed in C_{z_α} where the power effects predicted by the steady and quasi-steady tests were different from those predicted by perturbation tests.

The lateral parameters estimated by both the maximum likelihood and equation error methods generally showed the same trends with C_L. For C_{ℓ_β}, C_{ℓ_p}, $C_{\ell_{\delta a}}$, C_{n_β}, C_{n_p}, C_{n_r}, and $C_{n_{\delta r}}$ the values estimated using the two techniques agreed very well. The trends of the parameters estimated were as expected and the magnitudes determined were reasonable. As with the longitudinal results, the parameters estimated using maximum likelihood were considered the parameters to be used in any mathematical representation of the subject aircraft. The parameters C_{n_p} and $C_{n_{\delta a}}$ were correlated indicating that a description of the adverse yaw due to aileron input of this aircraft required a combination of these parameters.

The estimated parameter values obtained using the maximum likelihood extraction method resulted in fit errors less than the uncertainty in the measurements for both the longitudinal and lateral data. The estimated longitudinal parameters all had Cramer-Rao lower bounds that were less than 2 percent of their value, as did the lateral parameters C_{y_β}, C_{ℓ_β}, C_{ℓ_p}, $C_{\ell_{\delta a}}$, C_{n_β}, C_{n_r}, and $C_{n_{\delta r}}$. The lateral parameters C_{y_r}, $C_{y_{\delta r}}$, C_{ℓ_r}, and C_{n_p} had Cramer-Rao lower bounds that were less than 5 percent of the estimated parameter value, while $C_{\ell_{\delta a}}$ and $C_{n_{\delta a}}$ had bounds less than 10 percent of the value. C_{y_p} had a bound of approximately 25 percent of the extracted value.

The agreement of the two estimation methods, the reasonable trends and values of the extracted derivatives, the good fit to the data, and the low values of the Cramer-Rao lower bounds gave confidence that for the flight data examined, the mathematical model estimated using the maximum likelihood method was a reasonable representation of the subject aircraft.

REFERENCES

1. Wolowicz, Chester H.: Considerations in the Determination of Stability and Control Derivatives and Dynamic Characteristics From Flight Data. AGARD Rep. 549-Part 1, 1966.

2. Rampy, John M.; and Berry, Donald T.: Determination of Stability Derivatives From Flight Test Data by Means of High Speed Repetitive Operation Analog Matching. FTC-TDR-64-8, Air Force Flight Test Center, May 1964.

3. Howard, J.: The Determination of Lateral Stability and Control Derivatives From Flight Data. Canadian Aeronautics and Space Journal, vol. 13, March 1967, pp. 127-134.

4. Shinbrot, Marvin: On the Analysis of Linear and Nonlinear Dynamical Systems From Transient-Response Data. NACA TN 3288, 1954.

5. Grove, Randall D.; Bowles, Roland L.; and Mayhew, Stanley C.: A Procedure for Estimating Stability and Control Parameters From Flight Test Data by Using Maximum Likelihood Methods Employing a Real-Time Digital System. NASA TN D-6735, 1972.

6. Suit, William T.: Aerodynamic Parameters of the Navion Airplane Extracted From Flight Data. NASA TN D-6643, March 1972.

7. Cannaday, Robert L.; and Suit, William T.: Effects of Control Inputs on the Estimation of Stability and Control Parameters of a Light Airplane. NASA Technical Paper 1043, December 1977.

8. Klein, Vladislav: Determination of Stability and Control Parameters of a Light Airplane From Flight Data Using Two Estimation Methods. NASA TP 1306, 1979.

9. Fink, Marvin P.; Freeman, Delma C., Jr.; Greer, H. Douglas: Full-Scale Wind-Tunnel Investigation of the Static Longitudinal and Lateral Characteristics of a Light Single-Engine Airplane. NASA TN D-5700, 1970.

10. Greer, H. Douglas; Shivers, James P.; and Fink, Marvin P.: Wind-Tunnel Investigation of Static Longitudinal and Lateral Characteristics of a Full-Scale Mockup of a Light Single-Engine High-Wing Airplane. NASA TN D-7149, 1973.

11. Gerlach, O. H.: Determination of Performance, Stability and Control Characteristics From Measurement in Non-Steady Maneuvers. AGARD Specialists Meeting on Stability and Control, September 20-23, 1966, pp. 499-523.

12. Langdon, S. D.: Fixed-Wing Stability and Control Theory and Flight Test Techniques. USNTPS-FTM-No. 103, AD703681, August 1, 1969.

13. Klein, V.: Determination of Longitudinal Aerodynamic Derivatives From Steady-State Measurement of an Aircraft. Proceedings of the AIAA 4th Atmospheric Flight Mechanics Conference, Hollywood, Florida, August 8-10, 1977.

14. Iliff, Kenneth W.; and Maine, Richard E.: Practical Aspects of Using a Maximum Likelihood Estimation Method to Extract Stability and Control Derivatives From Flight Data. NASA TN D-8209, 1976.

15. Etkin, Bernard: Dynamics of Flight. John Wiley & Sons, Inc., c. 1959.

16. Roskam, Jan: Flight Dynamics of Rigid and Elastic Airplane. Roskam Aviator and Engineering Corp., c. 1972.

17. Smetana, Frederick O.; Summey, Delbert C.; and Johnson, W. Donald: Riding and Handling Qualities of Light Aircraft--A Review and Analysis. NASA CR-1975, 1972.

APPENDIX

EQUATIONS OF MOTION

The equations used in this program are perturbation equations from trimmed level flight and are written relative to the set of body axes shown in figure 1.

The equations used to describe the longitudinal motions were

$$\dot{u} = -qw + rv - g \sin \theta + \frac{1}{2} \rho \frac{V^2 S}{m}\left[C_{X,0} + C'_{X_\alpha}(\alpha - \alpha_t)\right] \tag{A1}$$

$$\dot{w} = -pv + qu + g \cos \theta \cos \varphi + \frac{1}{2} \rho \frac{V^2 S}{m}\left[C_{Z,o} + C'_{Z_\alpha}(\alpha - \alpha_t) + C_{Z_q} \frac{q\bar{c}}{2V} + C_{Z_{\delta e}}(\delta_e - \delta_{e,t})\right] \tag{A2}$$

$$\dot{q} = pr \frac{(I_Z - I_X)}{I_Y} + \frac{I_{XZ}}{I_Y}(r^2 - p^2) + \rho \frac{V^2 S\bar{c}}{2I_Y}\left[C_{m,o} + C_{m_\alpha}(\alpha - \alpha_t) + C_{m_{\dot{\alpha}}} \frac{\dot{\alpha}\bar{c}}{2V} + C_{m_q} \frac{q\bar{c}}{2V} + C_{m_{\delta e}}(\delta_e - \delta_{e,t})\right] \tag{A3}$$

$$\dot{\theta} = q \cos \varphi - r \sin \varphi \tag{A4}$$

$$a_X = \frac{1}{g}(\dot{u} + qw - rv + g \sin \theta) \tag{A5}$$

$$a_Z = \frac{1}{g}(\dot{w} + pv - qu - g \cos \theta \cos \varphi) \tag{A6}$$

$$V = \sqrt{u^2 + v^2 + w^2} \tag{A7}$$

$$\alpha = \tan^{-1} \frac{w}{u} \tag{A8}$$

$$\dot{\alpha} \approx \frac{\dot{w}}{u} \tag{A9}$$

$$C_{Z_{\delta e}} = \frac{\bar{c}}{l_t} C_{m_{\delta e}} \text{ (used in maximum likelihood extraction)} \tag{A10}$$

The values of the lateral states v, p, r, and φ used in the longitudinal equations were the flight-measured quantities.

Since thrust changes are not explicitly modeled in the equations of motion, C'_{X_α} and C'_{Z_α} are not necessarily pure C_{X_α} and C_{Z_α} but may contain small contributions due to changes in thrust. Therefore, C'_{X_α} and C'_{Z_α}, as determined in this study, are given by

$$C'_{X_\alpha} = \frac{\partial C_X}{\partial \alpha} + C_{T_\alpha} \cos \epsilon$$

$$C'_{Z_\alpha} = \frac{\partial C_Z}{\partial \alpha} + C_{T_\alpha} \sin \epsilon$$

Since, in this study, thrust was held constant and the angle-of-attack changes were no more than 7° peak to peak, the contributions of thrust to C'_{X_α} and C'_{Z_α} were considered minimal.

The equations used to compute the lateral motions were

$$\dot{v} = -ru + pw + g \cos \theta \sin \varphi + \frac{1}{2} \rho \frac{V^2 S}{m}\left[C_{Y,o} + C_{Y_\beta} \beta + C_{Y_p} \frac{pb}{2V} + C_{Y_{\delta r}}(\delta_r - \delta_{r,t})\right] \tag{A11}$$

$$\dot{p} = \frac{I_{XZ}}{I_X} \dot{r} + \left(\frac{I_Y - I_Z}{I_X}\right) qr + \left(\frac{I_{XZ}}{I_X}\right) pq + \frac{1}{2} \rho \frac{V^2 Sb}{I_X}\left[C_{l,o} + C_{l_\beta} \beta + C_{l_p} \frac{pb}{2V} + C_{l_r} \frac{rb}{2V} + C_{l_{\delta r}}(\delta_r - \delta_{r,t}) + C_{l_{\delta a}}(\delta_a - \delta_{a,t})\right] \tag{A12}$$

$$\dot{r} = \frac{I_{XZ}}{I_Z} \dot{p} + \left(\frac{I_X - I_Y}{I_Z}\right) pq - \left(\frac{I_{XZ}}{I_Z}\right) qr + \frac{1}{2} \rho \frac{V^2 Sb}{I_Z}\left[C_{n,o} + C_{n_\beta} \beta + C_{n_p} \frac{pb}{2V} + C_{n_r} \frac{rb}{2V} + C_{n_{\delta r}}(\delta_r - \delta_{r,t}) + C_{n_{\delta a}}(\delta_a - \delta_{a,t})\right] \tag{A13}$$

$$\dot{\varphi} = p + (q \sin \varphi + r \cos \varphi) \tan \theta \tag{A14}$$

$$a_Y = \frac{1}{g}(\dot{v} + ru - pw - g \cos \theta \sin \varphi) \tag{A15}$$

$$V = \sqrt{u^2 + v^2 + w^2}$$

$$\beta = \sin^{-1} \frac{v}{V}$$

The values of longitudinal states u, w, q, and θ used in the lateral equations were the flight-measured quantities. The equations were used to compute the airplane state responses. The computed responses were then compared with the recorded responses from the flight tests and the differences were used to update the parameters (stability and control derivatives) to improve the fit.

The longitudinal measured and computed responses, or states, used in the algorithm for this study were u, w, q, θ, a_X, and a_Z. The lateral states used were v, p, r, φ, and a_Y. Discussion of the identification algorithm is given in reference 7.

TABLE I.- GEOMETRIC CHARACTERISTICS

Mass, kg	837.93
Inertia:	
I_X, kg-m^2	1395.
I_Y, kg-m^2	1480.
I_Z, kg-m^2	2563.
I_{XZ}, kg-m^2	123.
Fuselage length, m	8.2
Wing:	
Area, m^2	16.2
Aspect ratio	7.47
Span, m	11.0
Mean geometric chord, m	1.49
Vertical tail:	
Area, m^2	1.04
Aspect ratio	3.96
Span, m	2.03
Rudder area, m^2	.68
Horizontal Tail:	
Area, m^2	3.35
Aspect ratio	3.44
Span, m	3.45
Tail length, m	4.36
α, β, V Boom location relative to c.g.:	
$\bar{x}$, m	1.47
$\bar{y}$, m	-5.43
$\bar{z}$, m	-.77

TABLE II.- INSTRUMENT RANGES

Instrument	Range
Airspeed, m/sec	0 to 63.0
Angle of attack, deg	-8.0 to 39.0
Angle of sideslip, deg	±23.0
Altitude, m	0 to
Normal acceleration, g units	-.5 to 4.0
Longitudinal acceleration, g units	±1.0
Lateral acceleration, g units	±1.0
Elevator position, deg	+25.0 to -29.0
Aileron position, deg	+16.0 to -20.0
Rudder position, deg	+19.0
Throttle position	Total Throttle travel
Pitch rate, deg/sec	±30.0
Roll rate, deg/sec	±30.0
Yaw rate, deg/sec	±30.0
Pitch attitude, deg	±30.0
Roll attitude, deg	±60.0

TABLE III.- FLIGHT TEST CONDITIONS

LONGITUDINAL

Trimmed Airspeed / Power Setting	31.6 m/sec	40.7 m/sec	54.2 m/sec
IDLE	1 run	2 runs	1 run
LEVEL FLIGHT	2 runs	2 runs	2 runs
FULL	2 runs	2 runs	same runs as Level Flight

LATERAL

Trimmed Airspeed / Power Setting	31.6 m/sec	31.6 m/sec	31.6 m/sec	31.6 m/sec
LEVEL FLIGHT	Input A 3 Runs	Input B 2 Runs	Input C 3 Runs	Input D 1 Run
Trimmed Airspeed / Power Setting	40.7 m/sec	40.7 m/sec	40.7 m/sec	40.7 m/sec
LEVEL FLIGHT	Input A 1 Run	Input B 3 Runs	Input C 2 Runs	Input D 1 Run
Trimmed Airspeed / Power Setting	54.2 m/sec	54.2 m/sec	54.2 m/sec	54.2 m/sec
LEVEL FLIGHT	Input A 2 Runs	Input B 3 Runs	Input C 3 Runs	Input D 1 Run

TABLE IV.- LONGITUDINAL PARAMETER VALUE

MAXIMUM LIKELIHOOD ESTIMATION METHOD
(CRAMER-RAO BOUNDS IN PARENTHESIS)

		AIRSPEED 31.6 m/sec →				
Power Setting		IDLE	TRIM	TRIM	FULL	FULL
Parameter						
C_{x_α}		1.68 (.0620)	1.40 (.0293)	1.41 (.0183)	1.44 (.0223)	1.81 (.0247)
C_{z_o}		-1.076 (.0024)	-.951 (.0017)	-.980 (.0030)	-1.00 (.0026)	-.972 (.0026)
C_{z_α}		-4.28 (.101)	-4.74 (.0622)	-4.92 (.0577)	-4.76 (.0841)	- 4.95 (.0670)
C_{z_q}		-9.77 (.969)	-9.78 (.754)	-10.29 (.714)	-13.09 (1.103)	-12.62 (.905)
$C_{z_{\delta e}}$		-.355	-.425	-.466	-.512	-.496
C_{m_α}		-1.22 (.0206)	-1.13 (.0110)	-1.06 (.0095)	-.862 (.0132)	-.947 (.0105)
$C_{m_{\dot\alpha}}$		-4.0*	-4.0*	-4.0*	-4.0*	-4.0*
C_{m_q}		-11.82 (.298)	-14.55 (.188)	-16.71 (.214)	-19.67 (.272)	-18.41 (.218)
$C_{m_{\delta e}}$		-1.04 (.0113)	-1.25 (.0071)	-1.37 (.0086)	-1.50 (.0102)	-1.45 (.0083)

*Parameter Fixed

LINEAR REGRESSION ESTIMATION METHOD

		AIRSPEED 31.6 m/sec →				
Power Setting		IDLE	TRIM	TRIM	FULL	FULL
Parameter						
C_{x_α}		1.58	1.46	1.50	1.60	1.56
C_{z_o}		-.954	-.866	-.888	-.89	-.87
C_{z_α}		-4.23	-4.74	-.477	-4.88	-4.85
C_{z_q}		-16.0	-13.71	-12.50	-18.98	-16.49
$C_{z_{qe}}$		-.43	-.39	-.34	-.56	-.44
C_{m_α}		-.963	-.927	-.916	-.744	-.815
$C_{m_q} + C_{m_\alpha}$		-17.36	-19.32	-19.20	-22.73	-21.50
$C_{m_{\delta e}}$		-1.02	-1.21	-.121	-1.39	-1.34

TABLE IV CONTINUED

MAXIMUM LIKELIHOOD ESTIMATION METHOD
(CRAMER-RAO BOUNDS IN PARENTHESIS)

	AIRSPEED 40.7 m/sec →					
Power Setting	IDLE	IDLE	TRIM	TRIM	FULL	FULL
Parameter						
C_{x_α}	1.22 (.0442)	1.01 (.0306)	.836 (.0169)	.867 (.0208)	.937 (.0174)	.884 (.0189)
C_{z_o}	-.641 (.0026)	-.665 (.0039)	-.645 (.0025)	-.612 (.0022)	-.639 (.0025)	-.614 (.0029)
C_{z_α}	-4.64 (.0838)	-4.56 (.0947)	-5.26 (.0472)	-5.07 (.0520)	-4.92 (.0636)	-4.98 (.0722)
C_{z_q}	-10.17 (1.091)	-10.76 (1.149)	-8.95 (.585)	-9.09 (.642)	-11.28 (.855)	-10.51 (.929)
$C_{z_{\delta e}}$	-.364	-.369	-.422	-.413	-.440	-.440
C_{m_α}	-.877 (.0114)	-.879 (.0155)	-.853 (.0086)	-.886 (.0078)	-.855 (.0098)	-.825 (.0118)
$C_{m_{\dot\alpha}}$	-4.0*	-4.0*	-4.0*	-4.0*	-4.0*	-4.0*
C_{m_q}	-13.00 (.248)	-13.51 (.319)	-14.94 (.245)	-14.75 (.171)	-15.92 (.228)	-15.87 (.296)
$C_{m_{\delta e}}$	-1.07 (.0090)	-1.08 (.0117)	-1.24 (.0103)	-1.21 (.0062)	-1.29 (.0087)	-1.29 (.0121)

*Parameter Fixed

LINEAR REGRESSION ESTIMATION METHOD

	AIRSPEED 40.7 m/sec →				
Power Setting	IDLE	TRIM	TRIM	FULL	FULL
Parameter					
C_{x_α}	.98	.85	.99	.94	.90
C_{z_o}	-.586	-.573	-.56	-.55	-.57
C_{z_α}	-4.72	-4.77	-4.72	-4.74	-.485
C_{z_q}	-16.8	-14.18	-16.27	-17.11	-15.39
$C_{z_{\delta e}}$	-.36	-.37	-.42	-.46	-.33
C_{m_α}	-.66	-.64	-.67	-.63	-.64
$C_{m_q} + C_{m_{\dot\alpha}}$	-17.76	-19.0	-19.5	-19.76	-20.14
$C_{m_{\delta e}}$	-1.04	-1.16	-1.17	-1.21	-1.23

TABLE IV CONCLUDED

MAXIMUM LIKELIHOOD ESTIMATION METHOD
(CRAMER-RAO BOUNDS IN PARENTHESIS)

	AIRSPEED 54.2 m/sec		
Power Setting	IDLE	FULL = TRIM	FULL = TRIM
Parameter			
C_{x_α}	.652 (.0244)	.52 (.0151)	.56 (.0221)
C_{z_o}	-.339 (.0024)	-.37 (.0027)	-.35 (.0025)
C_{z_α}	-5.02 (.0612)	-5.18 (.0672)	-5.27 (.0553)
C_{z_q}	-8.81 (.705)	-8.65 (.968)	-8.48 (.755)
$C_{z_{\delta e}}$	-.335	-.405	-.398
C_{m_α}	-.722 (.0130)	-.68 (.0101)	-.676 (.0101)
$C_{m_{\dot\alpha}}$	-4.0*	-4.0*	-4.0*
C_{m_q}	-12.30 (.301)	-15.34 (.337)	-15.35 (.318)
$C_{m_{\delta e}}$	-.98 (.0112)	-1.19 (.0134)	-1.17 (.0127)

*Parameter Fixed

LINEAR REGRESSION ESTIMATION METHOD

	AIRSPEED = 54.2 m/sec		
Power Setting	IDLE	FULL= TRIM	FULL= TRIM
Parameter			
C_{x_α}	.62	.54	.54
C_{z_o}	-.357	-.339	-.336
C_{z_α}	-.4.49	-4.64	-4.62
C_{z_q}	-19.54	-18.87	-19.56
$C_{z_{\delta e}}$	-.38	-.45	-.46
C_{m_α}	-.50	-.482	-.485
$C_{m_q} + C_{m_{\dot\alpha}}$	17.89	-19.86	-19.44
$C_{m_{\delta e}}$	-.985	1.13	-1.11

TABLE V.- THE PERCENT THE CRAMER-RAO BOUND IS OF THE ESTIMATED LONGITUDINAL PARAMETER

Power Setting	Airspeed	C_{x_α}	C_{z_o}	C_{z_α}	C_{z_q}	C_{m_α}	C_{m_q}	$C_{m_{\delta e}}$
TRIM	31.6 m/sec	3.690	0.223	2.360	9.918	1.689	2.521	1.087
TRIM	31.6 m/sec	2.093	0.179	1.312	7.710	0.932	1.292	0.568
TRIM	40.7 m/sec	1.298	0.306	1.173	6.939	0.896	1.281	0.628
TRIM	40.7 m/sec	1.549	0.260	1.767	8.426	1.531	1.383	0.680
TRIM	54.2 m/sec	1.365	0.267	1.354	7.171	1.109	1.184	0.641
TRIM	54.2 m/sec	3.623	0.406	1.806	10.728	1.300	1.908	0.841
FULL	31.6 m/sec	3.030	0.586	2.077	10.678	1.763	2.347	1.083
FULL	31.6 m/sec	2.022	0.388	0.897	6.536	1.008	1.640	0.831
IDLE	31.6 m/sec	2.399	0.359	1.026	7.063	0.880	1.159	0.512
FULL	40.7 m/sec	1.857	0.391	1.293	7.580	1.146	1.432	0.674
FULL	40.7 m/sec	2.138	0.472	1.450	8.839	1.430	1.865	0.938
IDLE	40.7 m/sec	3.742	0.708	1.219	8.002	1.801	2.447	1.143
IDLE	40.7 m/sec	2.903	0.730	1.297	11.191	1.485	2.197	1.126
IDLE	54.2 m/sec	3.946	0.714	1.049	8.903	1.494	2.072	1.085

TABLE VI.- PERIODS AND TIMES TO DAMP TO 1/2 AMPLITUDE

Flight condition	31.6 m/sec Trim power	31.6 m/sec Trim power	40.7 m/sec Trim power	40.7 m/sec Trim power	54.2 m/sec Full power	54.2 m/sec Full power	31.6 m/sec Full power
Extraction method	M.L.	Regression	M.L.	Regression	M.L.	Regression	M.L.
Period	1.80 sec	1.82 sec	1.58 sec	1.64 sec	1.26 sec	1.33 sec	1.94 sec
Time to damp to 1/2 amplitude	.295 sec	.268 sec	.235 sec	.217 sec	.174 sec	.160 sec	.262 sec

Flight condition	31.6 m/sec Full power	31.6 m/sec Idle power	31.6 m/sec Idle power	54.2 m/sec Idle power	54.2 m/sec Idle power
Extraction method	Regression	M.L.	Regression	M.L.	Regression
Period	1.90 sec	1.94 sec	1.91 sec	1.29 sec	1.36 sec
Time to damp to 1/2 amplitude	.241 sec	.372 sec	.271 sec	.197 sec	.173 sec

TABLE VII.- LATERAL PARAMETER VALUES DETERMINED USING MAXIMUM LIKELIHOOD ESTIMATION (CRAMER-RAO BOUNDS IN PARENTHESIS)

Case	20	21	22	23	24	25	26	27	28	29	30	31
Input	A	A	A	A	A	A	B	B	B	B	B	B
C_L	1.09	.975	1.102	.633	.388	.363	1.03	1.10	.67	.576	.562	.342
C_{y_β}	-.546 (.0036)	-.550 (.0045)	-.542 (.0030)	-.589	-.595 (.0049)	-.563 (.0042)	-.563 (.0056)	-.536 (.0060)	-.580 (.0034)	-.58 (.0052)	-.57 (.0086)	-.59 (.0037)
C_{y_p}	.058 (.0152)	.060 (.0208)	.027 (.0155)	-.089	-.041 (.0119)	-.081 (.0105)	.107 (.0172)	.140 (.0148)	.070 (.0108)	.053 (.0143)	.042 (.0288)	.054 (.0107)
$C_{y_{\delta r}}$	.150 (.0046)	.148 (.0071)	.160 (.0039)	.147	.130 (.0076)	.096 (.0052)	.152 (.0046)	.185 (.0045)	.166 (.0054)	.127 (.0047)	.145 (.0062)	.133 (.0042)
C_{ℓ_β}	-.057 (.00055)	-.059 (.00054)	-.058 (.00064)	-.070	-.071 (.0013)	-.073 (.00090)	-.061 (.00067)	-.062 (00071)	-.074 (.00047)	-.067 (.00067)	-.061 (.00089)	-.078 (.00055)
C_{ℓ_p}	-.405 (.0041)	-.400 (.0036)	-.438 (.0052)	-.430	-.404 (.0058)	-.44 (.0046)	-.44 (.0041)	-.439 (.0039)	-.484 (.0033)	-.440 (.0040)	-.391 (.0049)	-.477 (.0041)
C_{ℓ_r}	.0787 (.0021)	.100 (.0023)	.128 (.0023)	.090	.047 (.0045)	.079 (.0029)	.132 (.0022)	.137 (.0025)	.108 (.0020)	.101 (.0022)	.125 (.0027)	.078 (.0019)
$C_{\ell_{\delta r}}$	.00176 (.00041)	.0051 (.00045)	.0082 (.00045)	.0101	.0030 (.0013)	.0055 (.00060)	.0078 (.00041)	.012 (.0039)	.0077 (.00049)	.0058 (.00041)	.0110 (.00044)	.0079 (.00043)
$C_{\ell_{\delta a}}$	-.0742 (.00067)	-.081 (.00065)	-.089 (.00095)	-.096	-.095 (.0013)	-.098 (.00099)	-.101 (.00084)	-.100 (.00077)	-.114 (.00069)	-.104 (.00086)	-.087 (.00085)	-.114 (.00088)
C_{n_β}	.038 (.00042)	.038 (.00039)	.035 (.00045)	.039	.044 (.00034)	.042 (.00035)	.033 (.00033)	.038 (.00037)	.046 (.00020)	.042 (.00034)	.031 (.00052)	.051 (.00022)
C_{n_p}	-.139 (.0029)	-.104 (.0030)	-.124 (.0040)	-.104	-.062 (.0015)	-.071 (.0016)	-.108 (.0021)	-.117 (.0020)	-.058 (.0016)	-.078 (.0020)	-.144 (.0028)	-.031 (.0018)
C_{n_r}	-.121 (.0014)	-.117 (.0015)	-.109 (.0016)	-.101	-.098 (.0013)	-.095 (.0010)	-.144 (.0012)	-.124 (.0013)	-.100 (.00078)	-.113 (.0010)	-.132 (.0019)	-.105 (.00082)
$C_{n_{\delta r}}$	-.063 (.00034)	-.061 (.00037)	-.062 (.00032)	-.056	-.054 (.00037)	-.051 (.00032)	-.066 (.00035)	-.061 (.00036)	-.057 (.00028)	-.059 (.00030)	-.060 (.00043)	-.057 (.00024)
$C_{n_{\delta a}}$	-.011 (.00059)	-.0082 (.00058)	-.012 (.00078)	-.012	-.0061 (.00033)	-.0068 (.00037)	-.0015 (.00048)	-.0084 (.00044)	-.0011 (.00038)	-.0029 (.00042)	-.0134 (.00042)	.0019 (.00041)

TABLE VII.- CONTINUED

Case	32	33	34	35	36	37	38	39	40	41	42	43	44
Input	B	B	C	C	C	C	C	C	C	C	C	C	C
C_L	.320	.325	.326	.322	.326	.385	.376	.568	.662	.949	1.00	.988	.926
C_{y_β}	-.58 (.0037)	-.58 (.0036)	-.582 (.0037)	-.583 (.0035)	-.581 (.0036)	-.577 (.0033)	-.577 (.0030)	-.602 (.0040)	-.596 (.0032)	-.592 (.0054)	-.59 (.0032)	-.574 (.0026)	-.53 (.0044)
C_{y_p}	.0057 (.0148)	.041 (.0154)	-.122 (.0102)	-.092 (.0098)	-.116 (.0100)	-.025 (.0110)	-.011 (.0113)	-.181 (.0139)	-.122 (.0119)	-.070 (.0195)	-.079 (.0132)	-.032 (.0104)	.210 (.0141)
$C_{y_{\delta r}}$	.104 (.0057)	.121 (.0067)	.091 (.0054)	.111 (.0054)	.095 (.0054)	.114 (.0051)	.121 (.0044)	.134 (.0055)	.125 (.0050)	.178 (.0064)	.155 (.0042)	.139 (.0039)	.240 (.0075)
C_{ℓ_β}	-.087 (.00088)	-.081 (.00088)	-.074 (.00066)	-.074 (.00072)	-.072 (.00055)	-.081 (.00074)	-.082 (.00091)	-.069 (.00065)	-.0705 (.00069)	-.053 (.00066)	-.059 (.00042)	-.064 (.00041)	-.064 (.00059)
C_{ℓ_p}	-.557 (.0072)	-.505 (.0072)	-.461 (.0041)	-.457 (.0044)	-.456 (.0034)	-.49 (.0048)	-.485 (.0059)	-.448 (.0045)	-.442 (.0048)	-.377 (.0048)	-.416 (.0048)	-.445 (.0036)	-.45 (.0032)
C_{ℓ_r}	.047 (.0029)	.059 (.0037)	.076 (.0021)	.080 (.0026)	.071 (.0018)	.062 (.0022)	.078 (.0025)	.111 (.0020)	.093 (.0026)	.161 (.0028)	.124 (.0016)	.113 (.0016)	.128 (.0026)
$C_{\ell_{\delta r}}$	-.0005 (.00068)	.0045 (.00090)	.0035 (.00049)	.0060 (.00058)	.0023 (.00042)	.0036 (.00055)	.0094 (.00057)	.0083 (.00049)	.0087 (.00062)	.013 (.00065)	.0094 (.00045)	.0071 (.00042)	.0125 (.00057)
$C_{\ell_{\delta a}}$	-.127 (.0015)	-.117 (.0015)	-.103 (.00084)	-.105 (.00092)	-.102 (.00069)	-.114 (.0010)	-.115 (.0013)	-.102 (.00091)	-.103 (.0010)	-.094 (.0010)	-.099 (.00077)	-.103 (.00065)	-.114 (.00079)
C_{n_β}	.051 (.00030)	.051 (.00027)	.044 (.00022)	.044 (.00023)	.045 (.00019)	.049 (.00023)	.046 (.00027)	.040 (.00030)	.0404 (.00029)	.034 (.00041)	.038 (.00022)	.029 (.00024)	.034 (.00026)
C_{n_p}	-.028 (.0026)	-.030 (.0025)	-.063 (.0014)	-.053 (.0014)	-.061 (.0012)	-.037 (.0016)	-.055 (.0019)	-.090 (.0023)	-.086 (.0023)	-.095 (.0034)	-.067 (.0019)	-.130 (.0020)	-.073 (.0019)
C_{n_r}	-.101 (.0010)	-.111 (.0012)	-.096 (.00069)	-.093 (.00075)	-.096 (.00063)	-.100 (.00064)	-.101 (.00064)	-.099 (.00089)	-.104 (.0010)	-.125 (.0016)	-.137 (.00083)	-.139 (.00090)	-.094 (.0011)
$C_{n_{\delta r}}$	-.055 (.00028)	-.057 (.00032)	-.052 (.00029)	-.051 (.00029)	-.054 (.00026)	-.054 (.00023)	-.053 (.00021)	-.056 (.00032)	-.056 (.00031)	-.062 (.00045)	-.064 (.00026)	-.062 (.00025)	-.056 (.00027)
$C_{n_{\delta a}}$	.0014 (.00059)	.0029 (.00057)	-.0054 (.00030)	-.0037 (.00031)	-.005 (.00026)	+.0013 (.00036)	-.0035 (.00043)	-.0081 (.00053)	-.0075 (.00051)	-.00036 (.00077)	.0069 (.00045)	-.0064 (.00044)	.0015 (.00045)

TABLE VII.- CONCLUDED

Case	45	56
Input	D	D
C_L	.559	.320
C_{y_β}	-.56 (.0046)	-.59 (.0032)
C_{y_p}	.055 (.0143)	-.041 (.0084)
$C_{y_{\delta r}}$	.134 (.0074)	.131 (.0041)
C_{ℓ_β}	-.076 (.00095)	-.078 (.00073)
C_{ℓ_p}	-.47 (.0058)	-.47 (.0042)
C_{ℓ_r}	.080 (.0038)	.071 (.0025)
$C_{\ell_{\delta r}}$	.0114 (.00062)	.0097 (.00048)
$C_{\ell_{\delta a}}$	-.113 (.0012)	-.108 (.00090)
C_{n_β}	.043 (.00033)	.047 (.00021)
C_{n_p}	-.072 (.0024)	-.049 (.0013)
C_{n_r}	-.124 (.0015)	-.118 (.00079)
$C_{n_{\delta r}}$	-.065 (.00038)	-.058 (.00021)
$C_{n_{\delta a}}$	.00036 (.00052)	-.0015 (.00028)

TABLE VIII.- LATERAL PARAMETER VALUES DETERMINED USING LINEAR REGRESSION ESTIMATION

Case	20	21	22	23	24	25	26	27	28	29	30	31	32	33
Input	A	A	A	A	A	A	B	B	B	B	B	B	B	B
C_L	1.07	.975	1.102	.663	.388	.363	1.03	1.10	.67	.576	.562	.342	.32	.325
C_{y_β}	-.454	-.449	-.453	-.476	-.533	-.534	-.388	-.322	-.352	-.373	-.303	-.437	-.432	-.42
C_{y_p}	.0857	.046	.026	-.012	.033	.0202	.214	.349	.0864	.377	.666	.100	.034	.023
$C_{y_{\delta r}}$	.153	.110	.132	.119	.125	.127	.138	.137	.109	.0908	.102	.035	.011	.030
C_{ℓ_β}	-.0506	-.0518	-.0513	-.0608	-.0645	-.066	-.0476	-.047	-.0603	-.0637	-.054	-.075	-.077	-.075
C_{ℓ_p}	-.352	-.360	-.374	-.378	-.370	-.388	-.365	-.357	-.383	-.408	-.370	-.44	-.45	-.45
C_{ℓ_r}	.0834	.087	.102	.076	.0509	.045	.133	.129	.082	.115	.149	.077	.067	.076
$C_{\ell_{\delta a}}$	-.0697	-.0747	-.080	-.0873	-.088	-.091	-.0902	-.087	-.091	-.10	-.094	-.108	-.106	-.106
$C_{\ell_{\delta r}}$	.00062	.00166	.0038	.0049	.0031	.00466	.0093	.0087	.0043	.010	.015	.0095	.0074	.0087
C_{n_β}	.0334	.0318	.0336	.036	.0401	.0426	.026	.035	.036	.040	.047	.048	.048	.048
C_{n_p}	-.0912	-.087	-.0916	-.0708	-.0485	-.038	-.104	-.0745	-.0674	-.080	-.050	-.052	-.051	-.057
C_{n_r}	-.103	-.104	-.112	-.098	-.092	-.092	-.125	-.102	-.0985	-.127	-.110	-.117	-.119	-.123
$C_{n_{\delta a}}$	-.0081	-.0077	-.0072	-.0062	-.00309	-.00068	-.005	-.0013	-.0046	-.0044	-.0015	-.0034	-.0036	-.0036
$C_{n_{\delta r}}$	-.055	-.053	-.057	-.0512	-.0488	-.0477	-.057	-.053	-.050	-.061	-.058	-.058	-.058	-.059

TABLE VIII.- LATERAL PARAMETER VALUES DETERMINED USING LINEAR REGRESSION ESTIMATION (CONCLUDED)

Case	34	35	36	37	38	39	40	41	42	43	44	45	46
Input	C	C	C	C	C	C	C	C	C	C	D	D	D
C_L	.326	.322	.326	.385	.376	.568	.662	.949	1.00	.988	.926	.559	.320
C_{y_β}	-.508	-.516	-.509	-.502	-.515	-.500	-.49	-.447	-.452	.464	-.537	-.56	-.552
C_{y_p}	-.056	-.068	-.073	-.028	-.013	-.065	-.061	.085	.012	.081	.047	-.037	-.057
$C_{y_{\delta r}}$	.066	.073	.069	.082	.087	.124	.118	.155	.159	.144	.14	.082	.060
C_{ℓ_β}	-.076	-.075	-.076	-.076	-.077	-.071	-.071	-.057	-.058	-.064	-.060	-.073	-.083
C_{ℓ_p}	-.44	-.45	-.45	-.45	-.45	-.453	-.451	-.412	-.421	-.438	-.44	-.475	-.48
C_{ℓ_r}	.069	.072	.070	.071	.073	.096	.092	.145	.134	.117	.134	.094	.074
$C_{\ell_{\delta a}}$	-.106	-.106	-.106	-.108	-.109	-.108	-.108	-.102	-.104	-.105	-.111	-.115	-.114
$C_{\ell_{\delta r}}$	.0078	.0073	.0075	.0071	.0087	.0064	.0068	.0102	.0085	.0047	.012	.0075	.0103
C_{n_β}	.046	.046	.047	.046	.045	.042	.042	.034	.035	.029	.0302	.042	.047
C_{n_p}	-.054	-.049	-.0503	-.059	-.062	-.069	-.0709	-.094	-.086	-.126	-.101	-.078	-.056
C_{n_r}	-.114	-.116	-.115	-.12	-.118	-.118	-.119	-.138	-.14	-.143	-.111	-.122	-.127
$C_{n_{\delta a}}$	-.0031	-.0021	-.0025	-.0033	-.0045	-.0034	-.0041	-.0021	-.000046	-.0068	-.0045	-.0028	-.0029
$C_{n_{\delta r}}$	-.055	-.056	-.056	-.057	-.056	-.058	-.058	-.066	-.067	-.063	-.060	-.065	-.061

TABLE IX.- CHARACTERISTICS CALCULATED FROM ESTIMATED LATERAL PARAMETERS

MODE	C_L	ESTIMATION METHOD	PERIOD(SEC)	TIME TO HALF OR DOUBLE AMPLITUDE(SEC)
Dutch Roll	1.0	Maximum Likelihood	4.263	1.495
	1.0	Linear Regression	4.370	1.600
	.6	Maximum Likelihood	3.402	1.497
	.6	Linear Regression	3.416	1.522
	.35	Maximum Likelihood	2.598	1.337
	.35	Linear Regression	2.611	1.382
Roll	1.0	Maximum Likelihood	---	.162
	1.0	Linear Regression		.174
	.6	Maximum Likelihood		.122
	.6	Linear Regression		.126
	.35	Maximum Likelihood		.092
	.35	Linear Regression		.092
Spiral	1.0	Maximum Likelihood		43.95*
	1.0	Linear Regression		57.98*
	.6	Maximum Likelihood		81.27
	.6	Linear Regression		254.85
	.35	Maximum Likelihood		41.70
	.35	Linear Regression		46.00

*Time to double amplitude

TABLE X.- COMPARISON OF DERIVATIVE VALUES DETERMINED BY THE MAXIMUM LIKELIHOOD METHOD WITH THOSE FROM SELECTED REFERENCES

	Reference 10	Reference 17	Reference 16	Values from least squares' linear fit to the M.L. estimated parameters for three C_L values		
	$C_L = 1.1$	$C_L = .25$	$C_L = .9$	$C_L = .3$	$C_L = .6$	$C_L = 1.0$
C_{y_β}	- .54	- .22	- .303	- .59	- .57	- .55
C_{y_p}		- .047	- .213	- .045	- .005	.04
$C_{y_{\delta r}}$	.143	.15		.11	.14	.17
C_{ℓ_β}	- .0785	- .082	- .122	- .078	- .070	- .058
C_{ℓ_p}		- .47	- .494	- .47	- .45	- .41
C_{ℓ_r}		.07		.07	.095	.13
$C_{\ell_{\delta r}}$		.013		.0058	.007	.0095
$C_{\ell_{\delta a}}$	- .102	- .198		- .11	- .102	- .094
C_{n_β}	.057	.035	.0701	.048	.042	.033
C_{n_p}		- .077	- .096	- .05	- .078	- .115
C_{n_r}		- .062	- .115	- .10	- .11	- .125
$C_{n_{\delta r}}$	- .057	- .046		- .053	- 0.58	- .063
$C_{n_{\delta a}}$		.014		- .003	- .004	- .005

TABLE XI.- THE PERCENT THE CRAMER-RAO BOUND IS OF AN ESTIMATED LATERAL PARAMETER

PARAMETER	CASE NUMBER 20	21	22	24	25	26	27	28	29
C_{y_β}	0.659	0.818	0.554	0.824	0.746	0.995	1.12	0.586	0.897
C_{y_p}	26.21	34.67	57.41	29.02	12.96	16.07	10.57	15.43	26.98
C_{y_r}	3.220	4.692	2.507	5.800	3.937	4.305	3.963	3.00	3.890
$C_{y_{\delta r}}$	3.067	4.798	2.438	5.846	5.417	3.026	2.432	3.25	3.701
C_{ℓ_β}	0.965	0.915	1.103	1.831	1.233	1.098	1.145	0.635	1.00
C_{ℓ_p}	1.012	0.900	1.187	1.436	1.045	0.932	0.888	0.682	0.909
C_{ℓ_r}	2.668	2.300	1.797	9.574	3.671	1.667	1.825	1.852	2.178
$C_{\ell_{\delta r}}$	23.30	8.824	5.488	43.33	10.91	5.256	3.25	6.364	7.069
$C_{\ell_{\delta a}}$	0.903	0.802	1.067	1.368	1.010	0.832	0.770	0.605	0.827
C_{n_β}	1.105	1.026	1.286	0.773	0.833	1.000	0.974	0.435	0.810
C_{n_p}	2.086	2.885	3.226	2.419	2.254	1.944	1.709	2.759	2.564
C_{n_r}	1.157	1.282	1.468	1.327	1.053	0.833	1.048	0.780	0.885
$C_{n_{\delta r}}$	0.540	0.607	0.516	0.685	0.627	0.530	0.590	0.491	0.508
$C_{n_{\delta a}}$	5.364	7.073	6.500	5.410	5.441	32.000	5.238	34.55	14.48

TABLE XI.- CONTINUED

PARAMETER	CASE NUMBER 30	31	32	33	34	35	36	37	38
C_{y_β}	1.590	0.508	0.638	0.621	0.636	0.600	0.620	0.572	0.520
C_{y_p}	68.57	19.81	259.65	37.56	8.36	10.65	8.621	44.00	102.7
C_{y_r}	5.599	2.808	4.838	4.452	3.69	3.50	3.589	3.573	2.911
$C_{y_{\delta r}}$	4.276	3.158	5.481	5.537	5.93	4.775	5.579	4.474	3.636
C_{ℓ_β}	1.459	0.705	1.011	1.086	0.892	0.973	0.764	0.914	1.110
C_{ℓ_p}	1.253	0.860	1.293	1.426	0.889	0.963	0.746	0.980	1.196
C_{ℓ_r}	2.160	2.436	6.170	6.271	2.763	3.250	2.535	3.548	3.205
$C_{\ell_{\delta r}}$	4.000	5.443	136	20.0	14.00	9.667	18.261	15.28	6.064
$C_{\ell_{\delta a}}$	0.977	0.772	1.181	1.282	0.816	0.876	0.676	0.877	1.130
C_{n_β}	1.677	0.431	0.588	0.529	0.500	0.523	0.422	0.469	0.587
C_{n_p}	1.944	5.806	9.286	8.333	2.222	2.642	1.967	4.324	3.455
C_{n_r}	1.439	0.781	0.990	1.081	0.719	0.806	0.656	0.640	0.634
$C_{n_{\delta r}}$	0.717	0.421	0.509	0.561	0.538	0.549	0.481	0.426	0.396
$C_{n_{\delta a}}$	3.134	21.58	42.14	19.66	5.556	8.378	5.200	27.69	12.29

TABLE XI - CONCLUDED

PARAMETER	CASE NUMBER 39	40	41	42	43	44	45	46
C_{y_β}	0.664	0.536	0.912	0.542	0.453	0.830	0.821	0.542
C_{y_p}	7.680	9.754	27.86	16.71	32.5	6.714	26.00	20.49
C_{y_r}	3.584	3.972	4.337	3.673	3.164	5.41	9.609	3.733
$C_{y_{\delta r}}$	4.104	4.000	3.596	2.710	2.806	3.125	5.522	3.130
C_{ℓ_β}	0.942	0.979	1.245	0.712	0.641	0.922	1.250	0.936
C_{ℓ_p}	1.004	1.086	1.273	0.865	0.719	0.800	1.234	0.894
C_{ℓ_r}	1.802	2.796	1.739	1.290	1.416	2.031	4.750	3.521
$C_{\ell_{\delta r}}$	5.904	7.126	5.000	4.787	5.915	4.560	5.439	4.949
$C_{\ell_{\delta a}}$	0.892	0.971	1.064	7.778	0.631	0.693	1.062	0.833
C_{n_β}	0.750	0.718	1.206	0.579	0.828	0.765	0.767	0.447
C_{n_p}	2.556	2.674	3.579	2.836	1.538	2.603	3.333	2.653
C_{n_r}	0.899	0.962	1.280	0.606	0.647	1.170	1.210	0.670
$C_{n_{\delta r}}$	0.571	0.554	0.726	0.406	0.403	0.482	0.585	0.362
$C_{n_{\delta a}}$	6.543	6.800	213.89	6.522	6.875	30.000	144.4	18.67

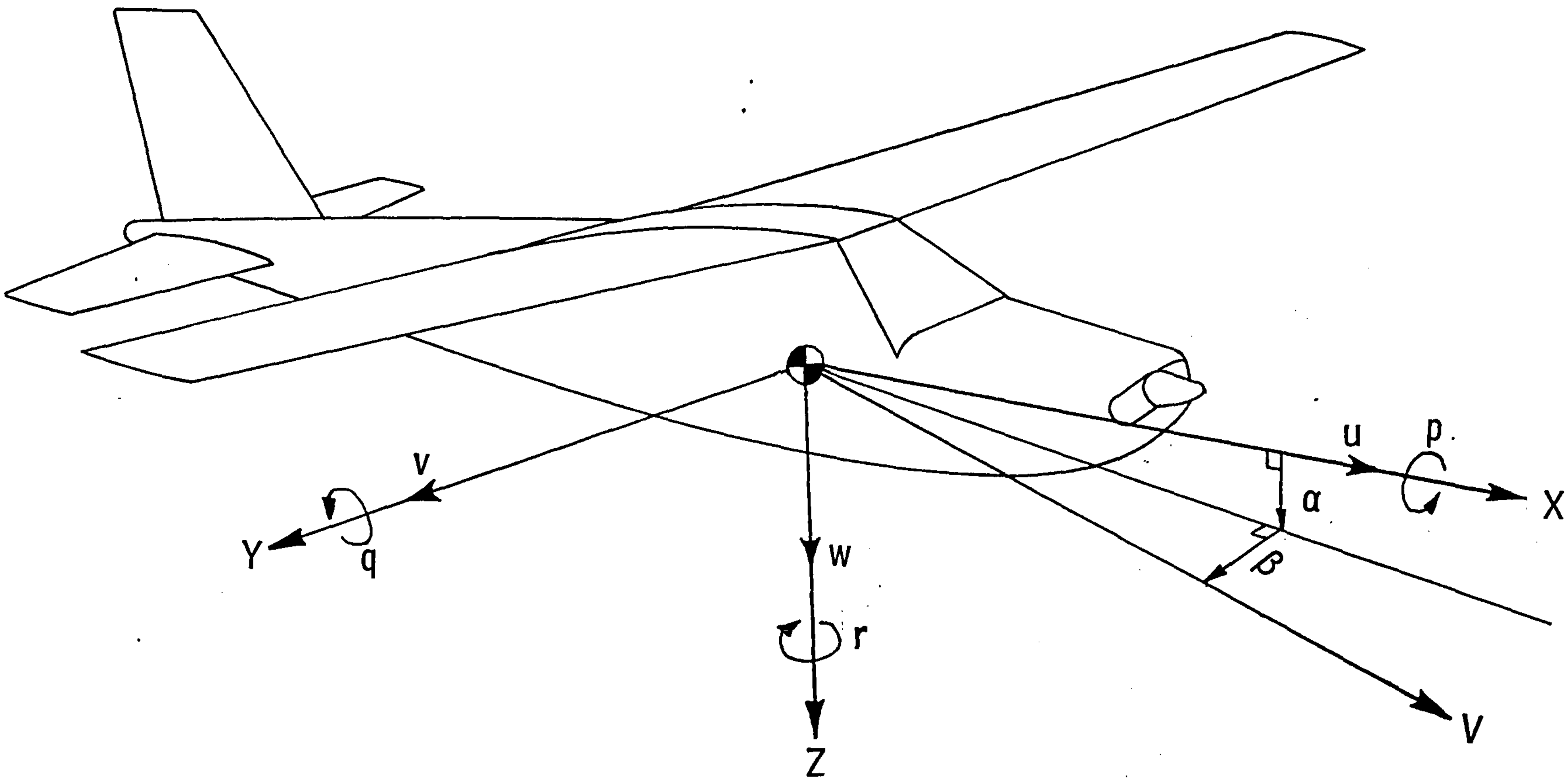

Figure 1.- System of body axes and positive sense of angles, forces, and moments.

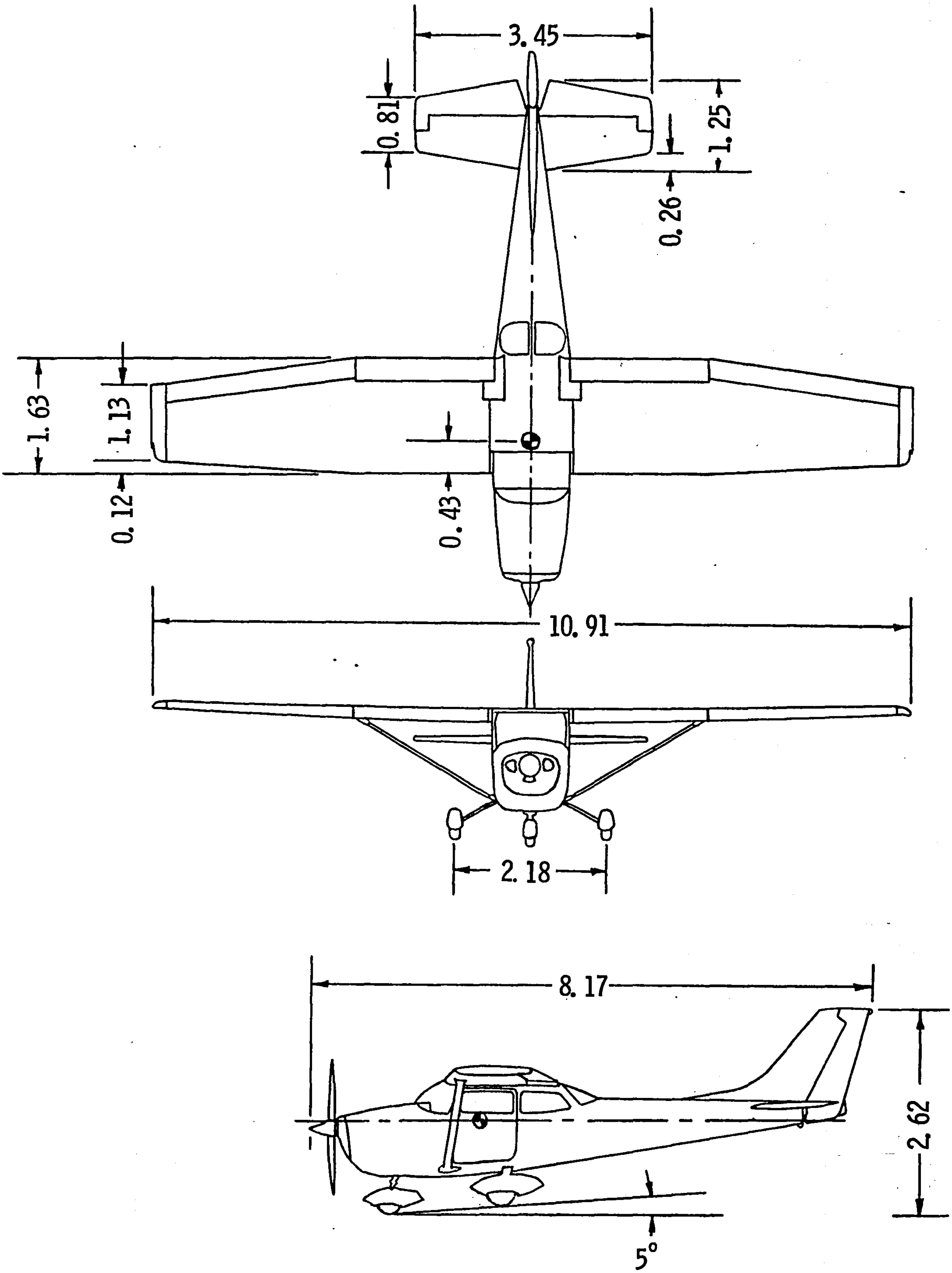

Figure 2.- Three-view drawing of the subject aircraft. All linear dimensions in meters.

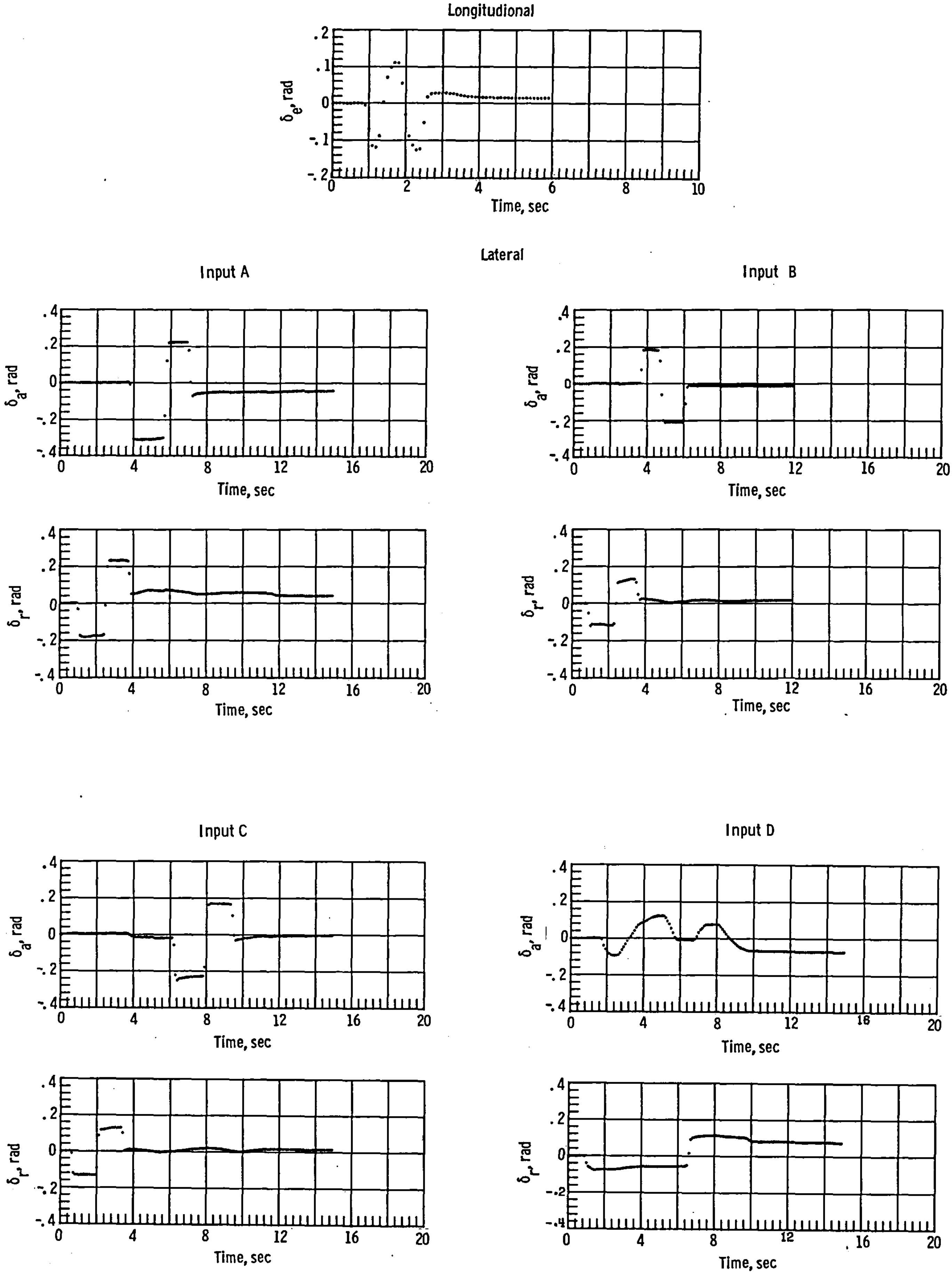

Figure 3. - Longitudinal and lateral control inputs.

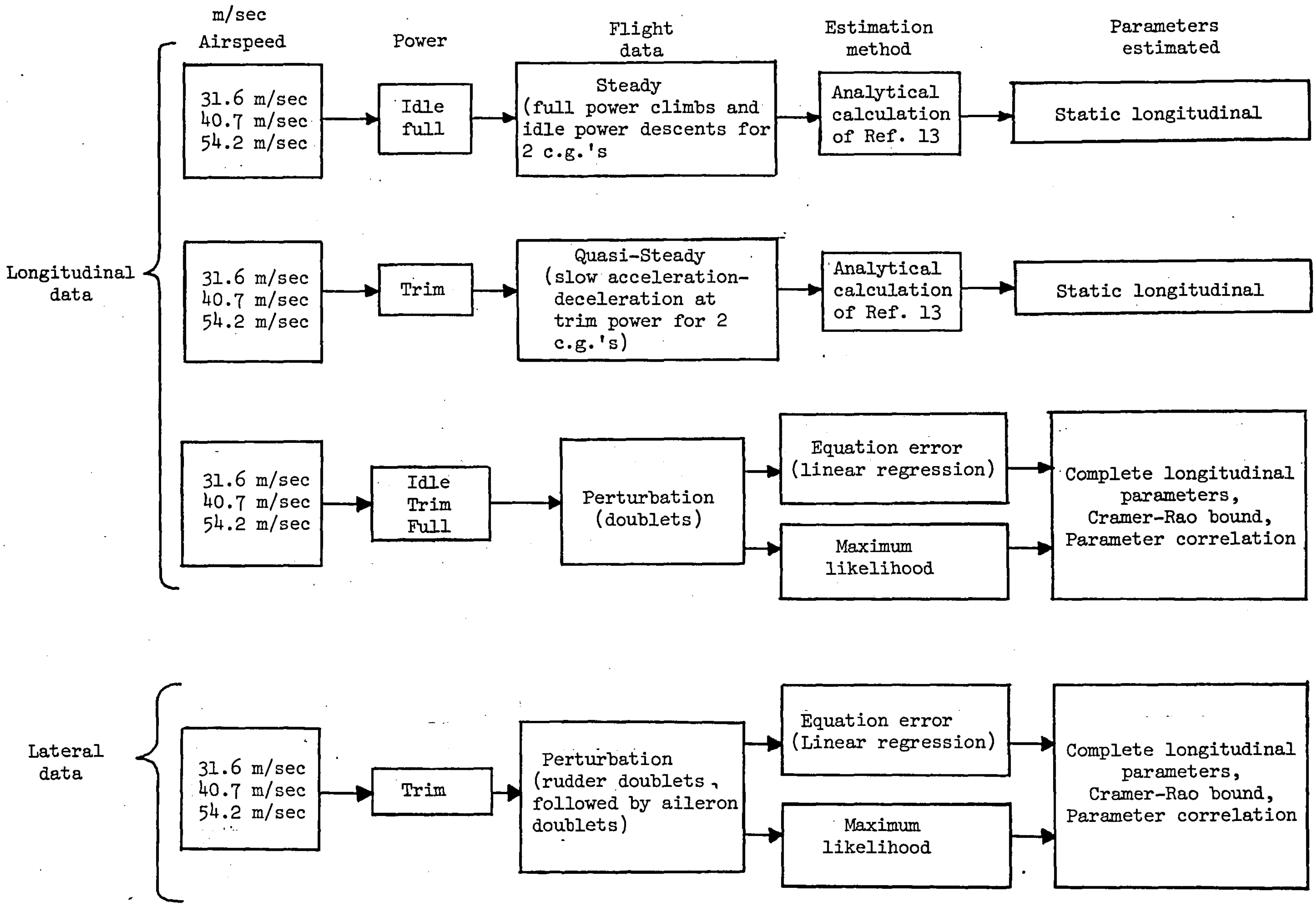

Figure 4.- Flight data processing scheme.

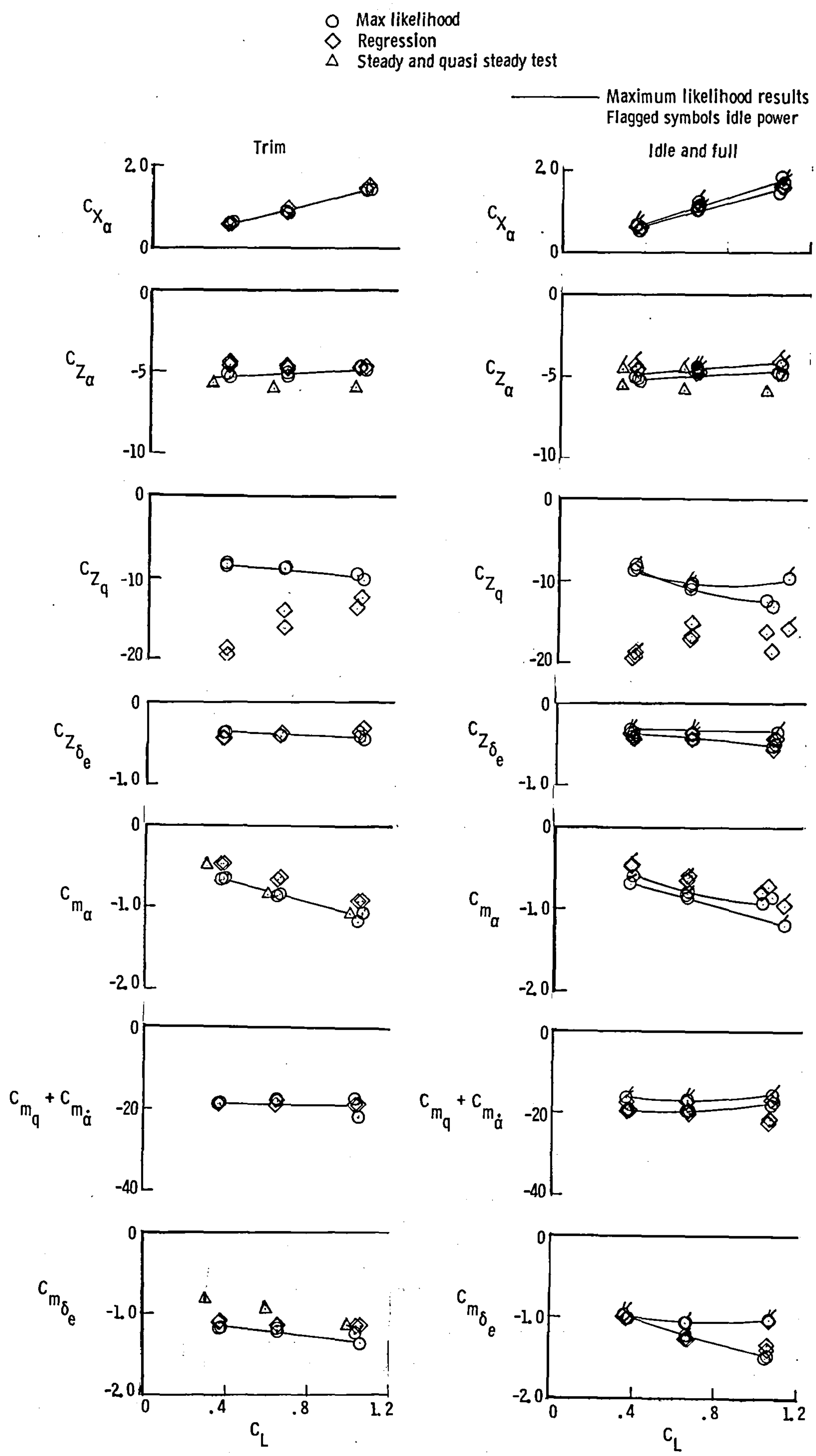

Figure 5. - Estimated longitudinal parameters versus C_L for three estimation methods.

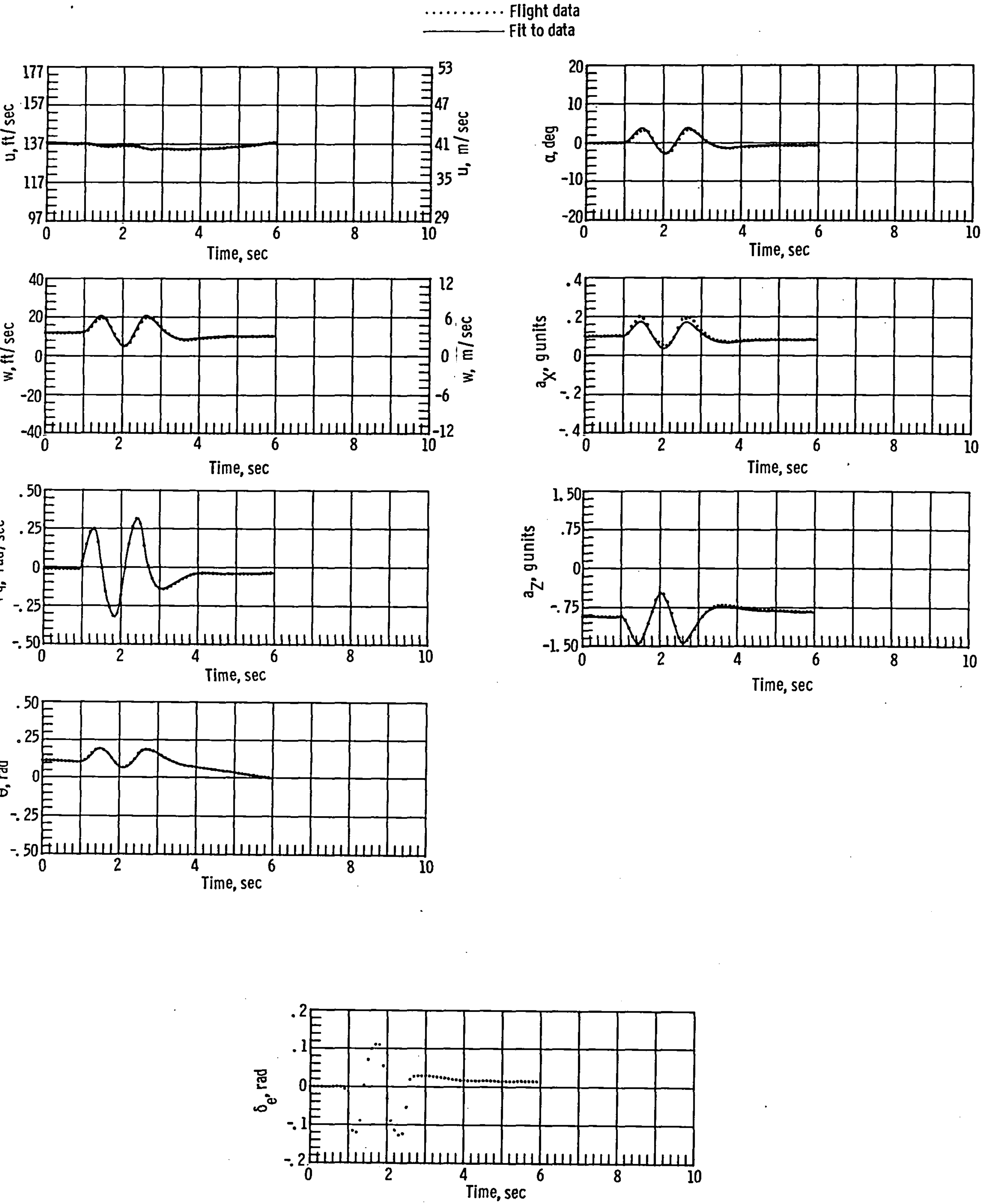

Figure 6. - Typical fits to responses to an elevator input.

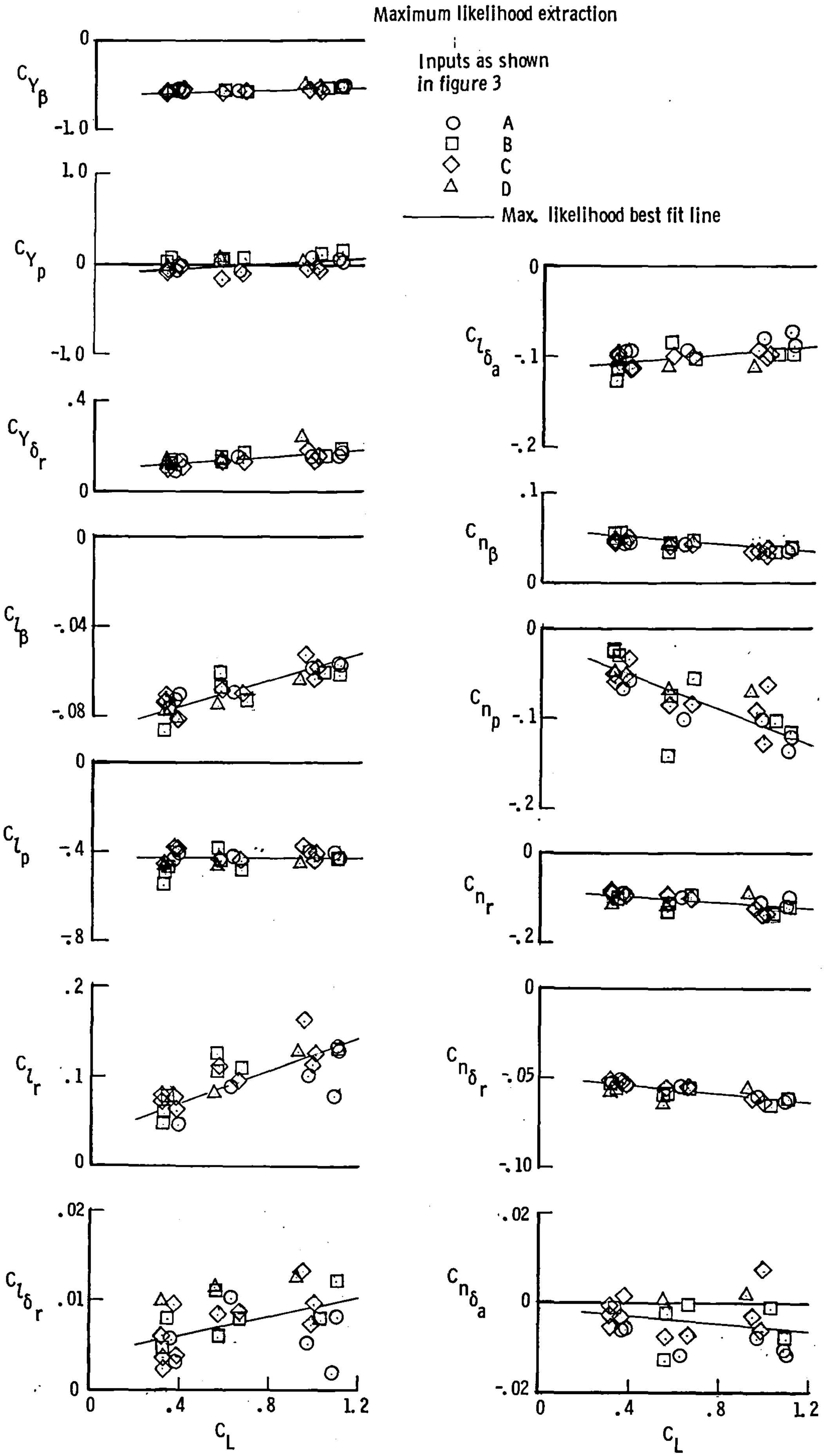

Figure 7. - Estimated lateral parameters determined using maximum likelihood versus C_L.

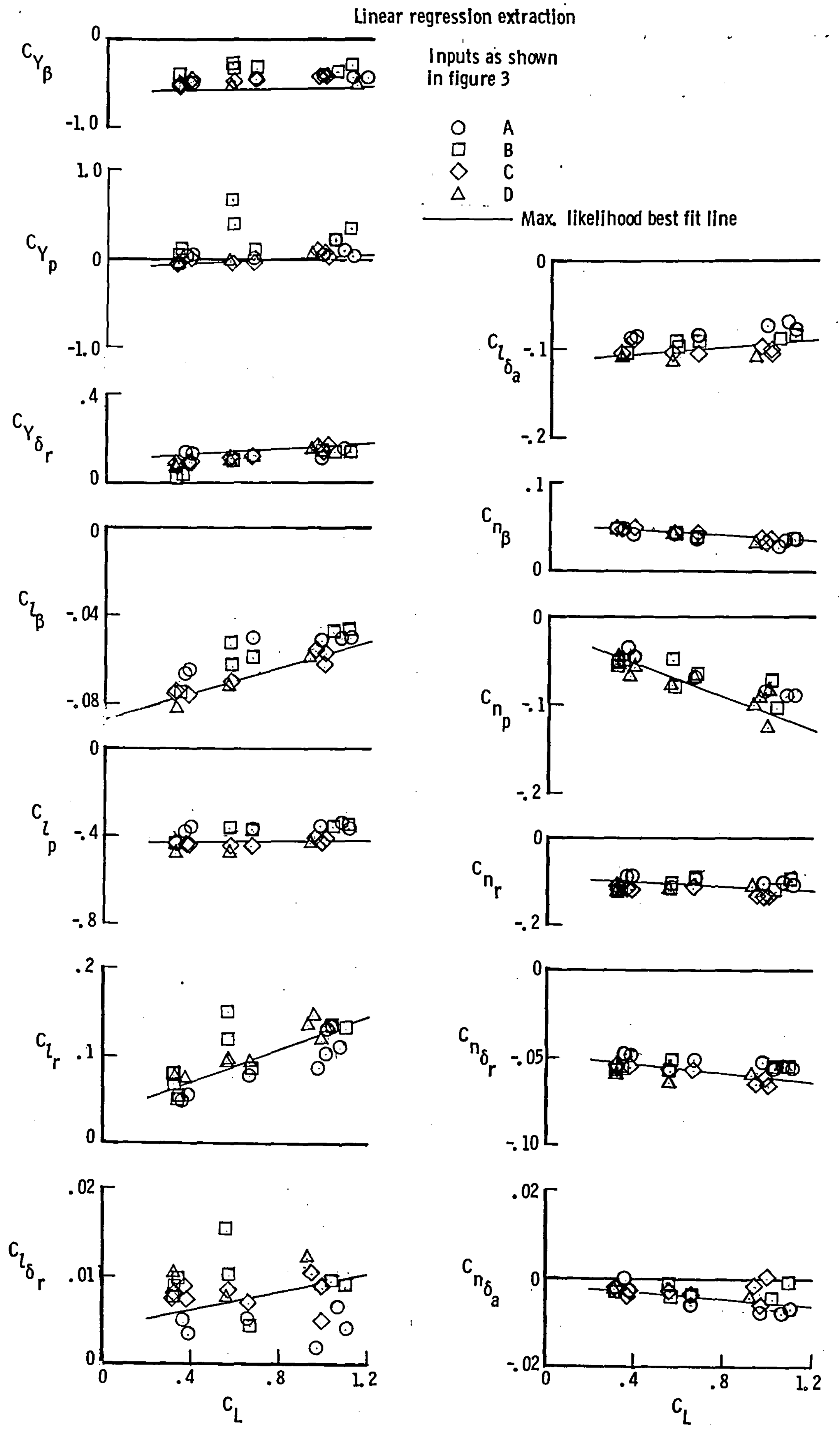

Figure 8. - Estimated lateral parameters determined using linear regression versus C_L.

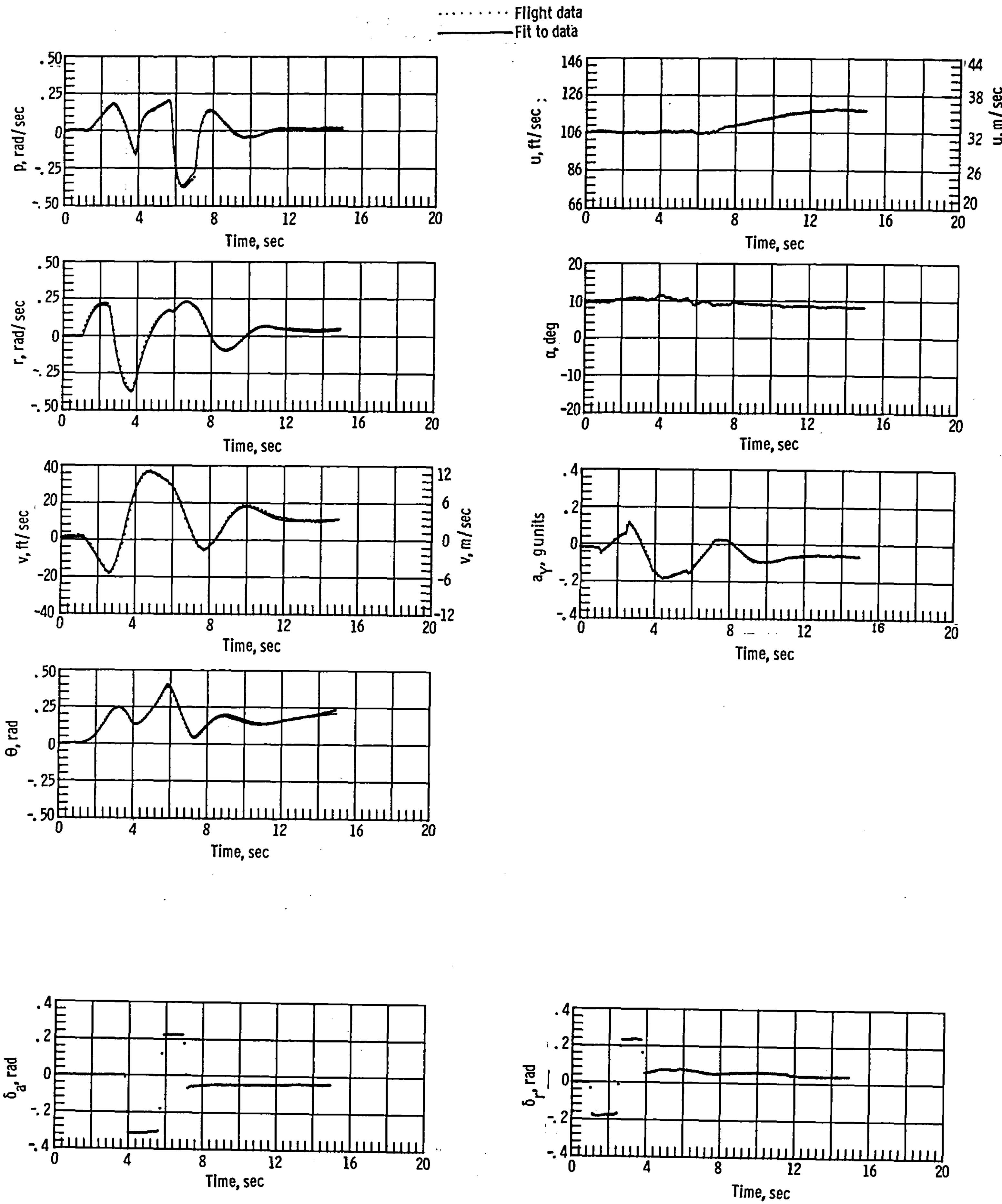

Figure 9. - Typical fits to responses to a rudder-aileron input.

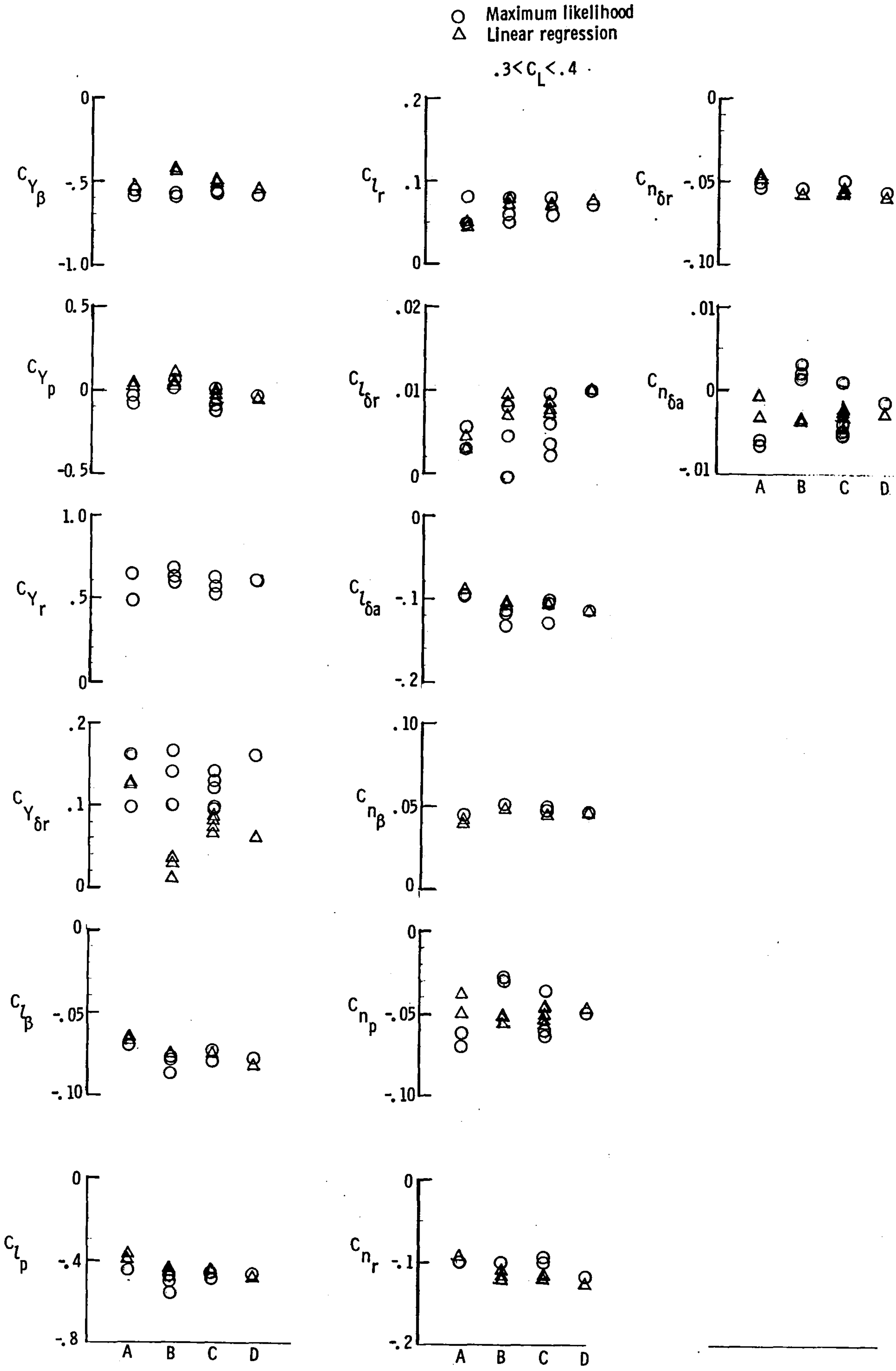

Figure 10. - Effect of control input form on estimated parameter values for the lateral inputs shown in figure 3.

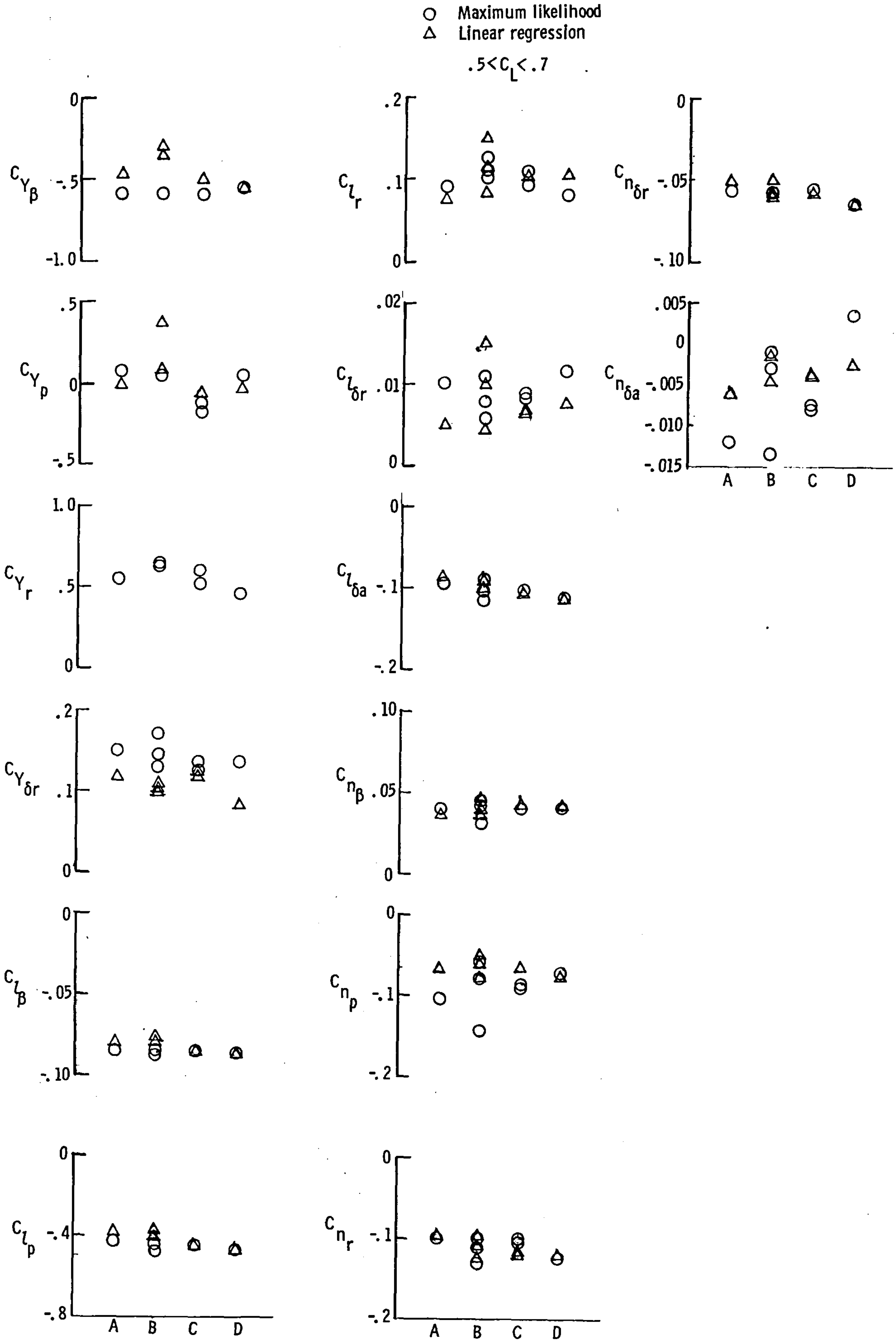

Figure 10. - Continued.

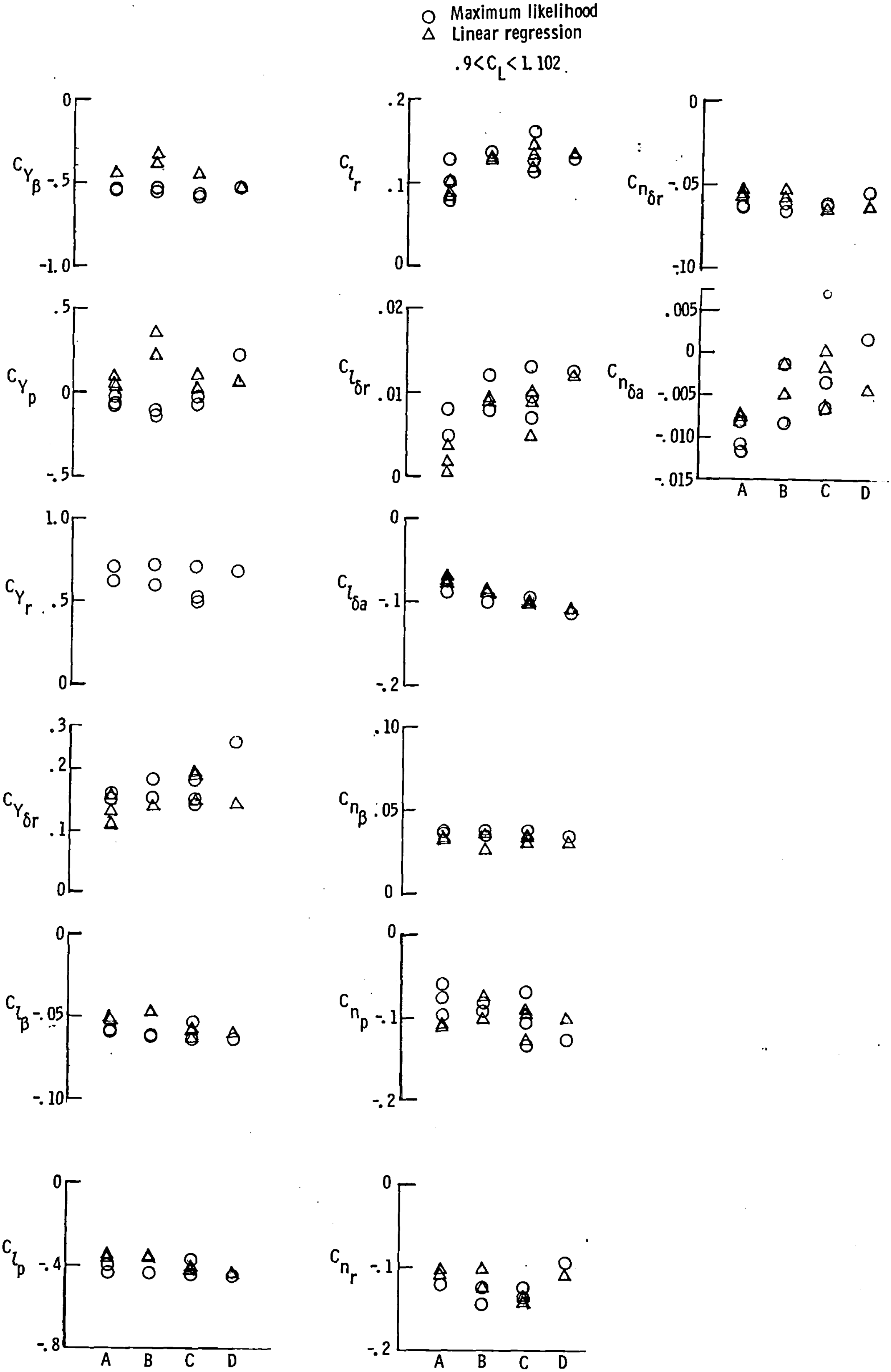

Figure 10. - Concluded.

1. Report No. NASA TM-80163	2. Government Accession No.	3. Recipient's Catalog No.
4. Title and Subtitle COMPARISON OF STABILITY AND CONTROL PARAMETERS FOR A LIGHT, SINGLE-ENGINE, HIGH-WINGED AIRCRAFT USING DIFFERENT FLIGHT TEST AND PARAMETER ESTIMATION TECHNIQUES		5. Report Date September 1979
		6. Performing Organization Code
7. Author(s) William T. Suit and Robert L. Cannaday		8. Performing Organization Report No.
		10. Work Unit No. 505-06-63-02
9. Performing Organization Name and Address NASA Langley Research Center Hampton, VA 23665		11. Contract or Grant No.
		13. Type of Report and Period Covered Technical Memorandum
12. Sponsoring Agency Name and Address National Aeronautics and Space Administration Washington, DC 20546		14. Army Project No.
15. Supplementary Notes		

16. Abstract

Longitudinal and lateral stability and control parameters were estimated from flight data for a high-wing, general aviation, airplane using flight data obtained at various flight conditions within the normal range of the aircraft. These parameters were estimated using an output error technique (maximum likelihood) and equation error technique (linear regression). Longitudinal static parameters were also estimated from climbing, descending, and quasi-steady-state flight data. For the lateral excitations, four input forms were used involving some combination of rudder and ailerons. The resulting longitudinal and lateral parameter estimates were used to compute the periods and time-to-damp to one-half amplitude of the various aircraft modes of motion to determine the sensitivity of these motions to variations in the parameter estimates.

17. Key Words (Suggested by Author(s))	18. Distribution Statement
Parameter estimation Stability and control parameters Maximum likelihood	Unclassified - Unlimited Subject Category 08

19. Security Classif. (of this report)	20. Security Classif. (of this page)	21. No. of Pages	22. Price*
Unclassified	Unclassified	52	$5.25

*For sale by the National Technical Information Service, Springfield, Virginia 22161